Accepted Manuscript

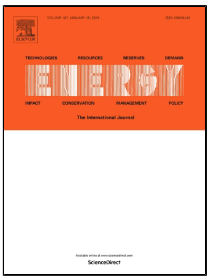

Melting and Solidification Characteristics of a Double-Pipe Latent Heat Storage System with Sinusoidal Wavy Channels Embedded in a Porous Medium

Amin Shahsavar, Abdullah A.A.A. Al-Rashed, Sajad Entezari, Pouyan Talebizadeh Sardari

PII:	S0360-5442(19)30047-7
DOI:	10.1016/j.energy.2019.01.045
Reference:	EGY 14518
To appear in:	*Energy*
Received Date:	25 October 2018
Accepted Date:	10 January 2019

Please cite this article as: Amin Shahsavar, Abdullah A.A.A. Al-Rashed, Sajad Entezari, Pouyan Talebizadeh Sardari, Melting and Solidification Characteristics of a Double-Pipe Latent Heat Storage System with Sinusoidal Wavy Channels Embedded in a Porous Medium, *Energy* (2019), doi: 10.1016/j.energy.2019.01.045

Melting and Solidification Characteristics of a Double-Pipe Latent Heat Storage System with Sinusoidal Wavy Channels Embedded in a Porous Medium

Amin Shahsavar[1], Abdullah A.A.A. Al-Rashed[2], Sajad Entezari[1], Pouyan Talebizadeh Sardari[3,*]

[1]Department of Mechanical Engineering, Kermanshah University of Technology, Kermanshah, Iran

[2]Department of Automotive and Marine Engineering Technology, College of Technological Studies, The Public Authority for Applied Education and Training, Kuwait

[3]Fluids and Thermal engineering research group, Faculty of Engineering, University of Nottingham, University Park, Nottingham, United Kingdom

* Corresponding authors

E-mails: pouyan.talebizadehsardari@nottingham.ac.uk (Pouyan Talebizadeh Sardari)

Abstract

The aim of this investigation is to explore the combined effects of porous medium and surface waviness on the melting and solidification of PCM inside a vertical double-pipe latent heat storage (LHTES) system. The results are compared with the cases of smooth channels and pure PCM. In the system, water is passed through the inner tube while composite PCM is placed in the annulus side. Different effective parameters including wavelength and wave amplitude of the sinusoidal wavy channels, porosity and pore size of the porous structure, Reynolds number and inlet temperature of water are examined to find the optimum geometric as well as operating conditions in both melting/solidification processes. The results show that utilizing both the high conductive porous structure and wavy channel reduces the melting/solidification times significantly. For the best case, the melting and solidification times of PCM reduce by 91.4% and 96.7%, respectively, compared with the smooth channels pure PCM system. The average rate of transferred heat for the wavy channel composite PCM are 10.4 and 18.9 times that for

the smooth channel pure PCM case. Comparing with the pure PCM system, the presence of copper foam reduces the effect of channel waviness significantly for both melting/solidification processes.

Keywords: Latent heat storage system; Phase change material; Porous medium; Sinusoidal wavy channel; Melting; Solidification.

Nomenclature

a_w	Wave amplitude (m)	$\dot{Q}$	Average rate of transferred heat (W)
A	Dimensionless wave amplitude	$s(y)$	Wave function
A_m	Mushy zone constant	$\vec{S}$	Source term in momentum equation
C	Inertial coefficient of porous medium	S_L	Source term in energy equation
$C_{p,f}$	Specific heat of PCM (J/kg.K)	t_m	Melting/solidification time (s)
$c_{p,por}$	Specific heat of porous medium (J/kg.K)	T	Temperature (K)
$c_{p,PCM}$	Specific heat of PCM (J/kg.K)	T_{ref}	Reference temperature (K)
d_p	Pore size (m)	$\vec{V}$	Velocity vector (m/s)
d_l	Ligament or cell diameter of the porous medium (m)	w	LHTES rate density (W)
g	Gravitational acceleration (m/s^2)	$\dot{W}$	Pumping power (W)
h	Sensible enthalpy (J/kg)		
h_{ref}	Sensible enthalpy at reference temperature (J/kg)	**Greek symbols**	
H	Total enthalpy (J/kg)	β_f	Thermal expansion coefficient (1/K)
k_e	Effective thermal conductivity (W/m.K)	ε	Porosity
k_f	Thermal conductivity of fluid (PCM) (W/m.K)	λ	Liquid fraction
k_s	Thermal conductivity of solid (porous material) (W/m.K)	μ_f	Dynamic viscosity (kg/m.s)
K	Permeability of porous medium (m^2)	ρ_f	Density (kg/m^3)
L	Dimensionless wavelength	$\rho_{f,ref}$	Density at reference temperature (kg/m^3)
L_w	Wavelength (m)	ω	Pore density (PPI)
L_f	Latent heat of fusion (J/kg)	ΔH	Latent heat (J/kg)
m_{pcm}	Mass of PCM (kg)	ΔP	Pressure drop (Pa)
m_{por}	Mass of porous medium (kg)		
p	LHTES rate (W)	**Subscripts**	
P	Pressure (Pa)	f	Fluid (PCM)
q	LHTES density (kJ)	s	Solid (metal foam)

Q	Heat storage capacity/total amount of transferred heat from PCM to water (kJ)	ref	Reference

1. Introduction

Latent heat thermal energy storage (LHTES), based on PCMs, is widely studied for energy storage applications due to a higher capacity (almost 5-14 times) compared with the sensible systems [1]. However, the drawbacks of low thermal conductivity of PCMs and the low rates of thermal diffusion within the PCMs, limit the employments of LHTES systems [2-4]. To solve these problems, a higher mass of PCMs should be utilized to provide the required amount of energy in a specified time which is not economically beneficial and increases the size of storage unit. Therefore, researchers have been tried to employ different methods to enhance the effective thermal conductivity of PCMs such as adding nanoparticles [5, 6] and/or to increase the rate of thermal diffusion inside the PCMs such as geometry modification [7, 8], using extended metal surfaces [9, 10], using encapsulated PCMs [11, 12] and employment of high conductive porous structures inside the PCMs [13-15].

Employment of high conductive porous structures have been demonstrated as one of the most efficient solutions for solving the drawbacks of pure PCMs [16]. In the presence of a porous medium, due to the higher conductivity of the porous medium than the pure PCM, the rate of conduction heat transfer enhances inside the PCM helping shorter melting/solidification process [17]. Py et al. [18] studied a composite paraffin-graphite matrix and presented that the equivalent thermal conductivity of the composite is ranged from 4 to 70 W/mK instead of 0.24 W/mK for the pure paraffin. They showed a reduction in the solidification time and higher stability of the LHTES system with the porous structure. Mesalhy et al. [19] performed a numerical analysis on the melting process of PCM embedded in a high conductivity porous matrix. They found a significant effect of the porous matrix on the rate of heat transfer and melting time. They claimed that although the melting rate increases by using the low porosity

medium, due to reducing the convection effect, a PCM storage with high porosity and high thermal conductivity is the best technique. Mahdi et al. [20] studied a triplex-tube LHTES system using both nanoparticles and metal foam to increase the melting time of the heat exchanger. They reported that by using the copper porous medium with 95% porosity, the melting time reduces by 88.8% and 89.5% without and with 5% alumina nanoparticles, respectively, which shows the negligible effect of nanoparticles in the presence of porous medium. Without the porous foam, the presence of 5% nanoparticles resulted in just 19.7% reduction in the melting time. Therefore, they proved the advantage of adding high conductive porous foams rather than nanoparticles to overcome the heat transfer problem in LHTES systems. Zhang et al. [21] numerically evaluated a composite metal foam/PCM using either copper or nickel as the porous material with the porosity of 97% and molten salt as the PCM for solar energy storage utilization. They showed the better performance of copper metal foam than Nickel which reduce the melting time by 28.3% compared with the pure PCM case. Esapour et al. [22] studied melting and solidification in a horizontal multi-tube heat storage system using a composite metal foam/PCM. They investigated different number of inner tubes with various locations on the melting and solidification times. They showed that for the best case, the melting and solidification times are reduced by 48% and 72%, respectively.

One of the promising methods for heat transfer enhancement between two fluids in heat exchangers is using wavy walls instead of smooth walls at the locations of heat transfer [23-25]. It has been shown that in the presence of wavy channels, higher efficiency and higher heat transfer performance of the heat exchanger can be achieved [26, 27]. Literature survey shows that there are only two studies which have analysed the effect of wavy channels on the performance of LHTES systems. Kashani et al. [28] performed an analysis on the solidification of Cu-water nanofluid in a 2-D cavity with vertically wavy walls. They showed that the solidification time can be controlled by using the surface waviness which can enhance the heat

transfer performance in the domain. Abdollahzadeh and Esmaeilpour [29] studied the solidification of Cu-water nanofluid in a vertical enclosure with different sinusoidally curved wavy surfaces including divergent-convergent and convergent-divergent walls for different Grashof numbers. They proved the higher rate of heat transfer using sinusoidal wavy walls. They claimed that although the use of nanoparticles reduces the solidification time; however, it also decreases the capacity of thermal energy storage/release. Therefore, channel waviness was recommended to improve the performance of PCM without reducing the heat storage capacity.

Geometry modification is employed widely in the literature due to the possible combination with other methods. Agyenim et al. [30] conducted experiments to compare the temperature distribution of horizontal shell and tube heat exchangers with one and four heat transfer tubes and showed higher temperature gradients using multiple heat transfer tubes instead of one. Esapour et al. [8] analysed the effects of inner tubes number, heat transfer fluid (HTF) mass flow rate and temperature on the performance of a horizontal multi-tube cylindrical LHTES system. They showed that increasing the number of inner tubes from 1 to 4 with the same volume of the PCM results in a 29% reduction in the melting time. Wang et al. [31] studied a zigzag plate configuration of an air-PCM heat exchanger using multi-PCMs (m-PCMs) with different melting points and unequal mass ratios. They found that the charging process is affected significantly by the use of m-PCMs compared with a single PCM.

The objective of this paper is to positively combine wavy channel/metal foams effects as a hybrid heat transfer enhancement method to improve the PCM melting and solidification processes in a vertical double-pipe LHTES system (LHTES-W) compared with the system with smooth walls (LHTES-S). Different effective parameters of the channel waviness including the wavelength and wave amplitude, porous structure including the porosity and pore size, and HTF including the Reynolds number and inlet temperature are investigated according to the

melting/solidification time, rate of heat transfer and pumping power. The liquid fraction and temperature distributions are well examined to display the advantageous effect of the proposed LHTES-W unit. To the best knowledge of the authors, this assessment is unique since it contributes for the first time the results of the performance of a LHTES-W system that houses PCM infiltrated metal foams. The proposed LHTES system in this study could provide guidelines for the combination of different heat transfer enhancement methods for reducing the melting and solidification times and improving the energy efficiency of the system.

2. Mathematical modelling

In a pure PCM, heat is transferred to the solid PCM by conduction and then spread out in the liquid PCM by convection and conduction. To increase the heat transfer inside the PCM, a porous foam is prepared and the PCM is injected into the porous media [18]. The heat is more transferred by the high conductivity solid porous medium through the PCM. In the numerical modelling of PCM, to consider the effect of phase change, the enthalpy-porosity model is used where the porosity is set equal to the liquid fraction in each cell. In the presence of porous medium, in addition to the pressure drop caused by the solidified materials, a pressure loss is considered due to the viscous and inertial losses in the momentum equation [32]. The following assumptions are made in the present numerical investigation [20, 33]:

- The liquid phase is considered as an incompressible Newtonian fluid.
- To consider the variation of density, Boussinesq approximation is applied due to small temperature gradient in the domain and the flow is considered laminar.
- The porous medium is considered homogeneous and isotropic.
- The thermal equilibrium thermal model is used for the energy equation.
- The volume expansion of the PCM is neglected during phase change.
- Viscous dissipation is negligible.

- Flow is modelled as 2D axisymmetric due to the geometry of the double-pipe and since there is not circumferential variation in the flow.

Therefore, the governing equations are given as [21]:

Continuity:

$$\frac{\partial \rho_f}{\partial t} + \nabla . \rho_f \vec{V} = 0 \tag{1}$$

Momentum:

$$\frac{\rho_f \partial \vec{V}}{\varepsilon\ \partial t} + \frac{\rho_f}{\varepsilon^2}(\vec{V}.\nabla)\vec{V} = -\nabla P + \frac{\mu_f}{\varepsilon}(\nabla^2 \vec{V}) - \rho_{f,ref}\beta_f \varepsilon (T - T_{ref})\vec{g} - \vec{S} - \vec{F} \tag{2}$$

Energy:

$$\frac{\partial \varepsilon \rho_f C_{p,f} T}{\partial t} + \nabla\left(\rho_f C_{p,f} \vec{V} T\right) = \nabla(k_e \nabla T) - S_L \tag{3}$$

As mentioned, it is assumed that a local thermal equilibrium exists between the PCM and the metal foam. It means that, at any time, temperature of the PCM is equal to the temperature of the metal foam at any representative control volume and therefore, one equation is just considered as the energy equation for both the PCM and metal foam. In the thermal equilibrium model, the volume average of the conductivities of metal foam and PCM is considered as the effective thermal conductivity of the composite PCM given as [33]:

$$k_e = (1 - \varepsilon)k_s + \varepsilon k_f \tag{4}$$

Note that the Boussinesq approximation is used by the term of $\rho_{f,ref}\beta_f(T - T_{ref})\vec{g}$ which is added to the momentum equation in the gravity direction to consider the effect of density variation [20]. Besides, the source terms in the momentum equation are related to the pressure drop due to the effect of phase change which are defined according to the Darcy's law of damping and are given as [20]:

$$\vec{S} = A_m \frac{(1 - \lambda)^2}{\lambda^3 + 0.001}\vec{V} \tag{5}$$

where A_m is the mushy zone constant usually within the range of 10^4-10^7. In the current study, A_m is assumed constant equal to 10^5 [34-36]. Note that for the pure PCM, in the governing equations, the porosity is equal to 1 and the source terms due to the presence of porous media are omitted from the momentum equations. For the water, in addition to consider 1 for the porosity, A_m is considered zero to eliminate the effect of phase change.

Additionally, λ is defined as [9]:

$$\lambda = \frac{\Delta H}{L_f} = \begin{cases} 0 & if \;\; T < T_{Solidus} \\ 1 & if \;\; T > T_{Liquidus} \\ \dfrac{T - T_{Solidus}}{T_{Liquidus} - T_{Solidus}} & if \;\; T_{Solidus} < T < T_{Liquidus} \end{cases} \tag{6}$$

where ΔH may vary between zero for solid and L_f for liquid.

The total enthalpy is the summation of sensible and latent heat given as:

$$H = h + \Delta H \tag{7}$$

where h is defined as follows:

$$h = h_{ref} + \int_{T_{ref}}^{T} Cp_f dT \tag{8}$$

The last term on the right-hand side of the momentum equations are due to the presence of the porous medium and are calculated as:

$$\vec{F} = \left(\frac{\mu_f}{K} + \frac{\rho_f C|\vec{V}|}{\sqrt{K}}\right)\vec{V} \tag{9}$$

In the above equations, the first term is the viscous loss term and the second term is the inertial loss term. In these equations, K and C are given as [32]:

$$K = 0.00073{d_p}^2(1-\varepsilon)^{-0.224}\left(\frac{d_l}{d_p}\right)^{-1.11} \tag{10}$$

$$C = 0.00212(1-\varepsilon)^{-0.132}\left(\frac{d_l}{d_p}\right)^{-1.63} \tag{11}$$

where d_l is obtained as:

$$d_l = 1.18 d_p \sqrt{\frac{1-\varepsilon}{3\pi}} \left(\frac{1}{1 - e^{-(1-\varepsilon)/0.04}} \right) \quad (12)$$

and d_p is calculated as:

$$d_p = 0.0254/\omega \text{ (PPI)} \quad (13)$$

where ω is defined in terms of PPI means the number of pores per inch.

The source term in the energy equation is given as [31]:

$$S_L = \frac{\partial \varepsilon \rho_f \lambda L_f}{\partial t} + \nabla \left(\rho_f \vec{V} \lambda L_f \right) \quad (14)$$

To evaluate the performance of the LHTES unit, in addition to the melting/solidification time and rate of heat transfer to/from the PCM, three different parameters including the LHTES rate, LHTES density and LHTES rate density are considered. LHTES rate is the ratio of the capacity of storage unit to the melting/solidification time given as [37]:

$$p = \frac{Q}{t_m} = \frac{m_{por} \int c_{p,por} dT + m_{pcm} \left(\int_{solid} c_{p,pcm} dT + L_f + \int_{liquid} c_{p,pcm} dT \right)}{t_m} \approx \frac{m_{pcm} L_f}{t_m} \quad (15)$$

The LHTES density is the ratio of the storage unit capacity to the mass of the composite material given as [37]:

$$q = \frac{Q}{m} = \frac{m_{por} \int c_{p,por} dT + m_{pcm} \left(\int_{solid} c_{p,pcm} dT + L_f + \int_{liquid} c_{p,pcm} dT \right)}{m_{por} + m_{pcm}} \approx \frac{m_{pcm} L_f}{m_{por} + m_{pcm}} \quad (16)$$

Since the sensible heat is greatly smaller than the latent heat and also latent heat is the most important parameter in the LHTES capacity, just the latent heat is usually considered for the calculating the LHTES performance.

To consider the effects of storage capacity, melting/solidification time and mass of the materials all together, LHTES rate density is defined by Ref. [37] as the ratio of heat storage capacity to the melting/solidification time and mass of the composite material given as:

$$w = \frac{Q}{t_m m} = \frac{m_{por}\int c_{p,por}dT + m_{pcm}\left(\int_{solid} c_{p,pcm}dT + L_f + \int_{liquid} c_{p,pcm}dT\right)}{t_m(m_{por} + m_{pcm})} \approx \frac{m_{pcm}L_f}{t_m(m_{por} + m_{pcm})} \quad (17)$$

3. Geometry, Boundary conditions and PCM properties

The schematic of the geometry is illustrated in Fig. 1. It is a vertical double-pipe LHTES system with a wavy wall with the dimensions of 25 cm for the length, 4 cm and 8cm for the inner and outer diameters, respectively. The wall thickness of the inner tube is considered to be 1 mm. The shape of the wavy wall profile is defined by:

$$s(y) = a_w sin\left(\frac{2\pi y}{L_w}\right) \quad (18)$$

a_w and L_w are shown in Fig. 1. Note that in the following, the dimensionless wavelength (L) and dimensionless wave amplitude (A) are used which are equal to the ratio of wavelength and wave amplitude to the width of the PCM zone, respectively.

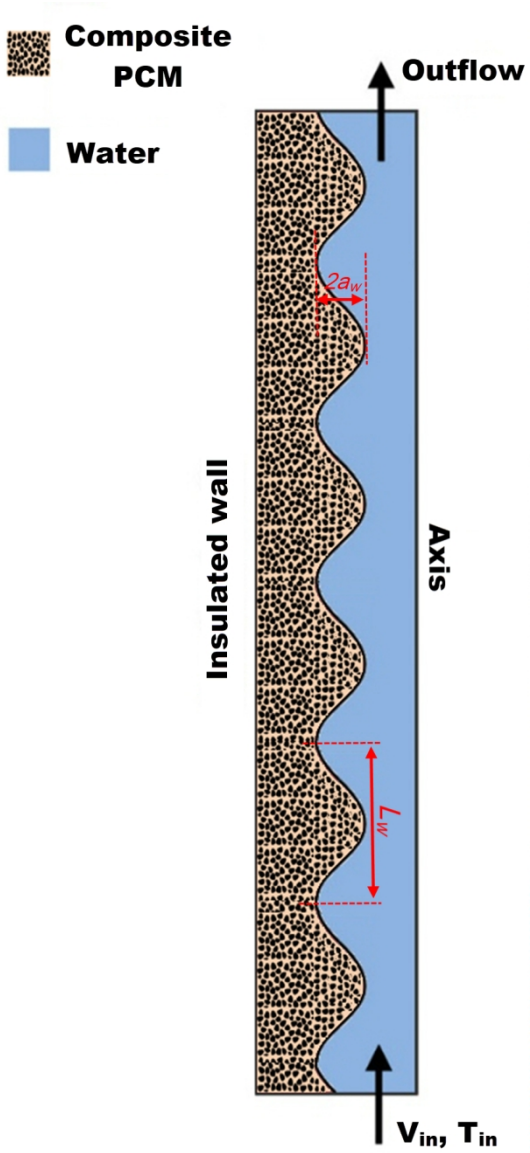

Fig. 1. Schematic of the studied double-pipe LHTES system.

The laminar flow of water is passed through the inner tube while the PCM embedded in the copper foam fills the annulus. Uniform velocity and uniform temperature are assumed at the tube inlet. The outflow boundary condition is applied to the tube outlet and the no-slip boundary condition is defined for the walls. The PCM is insulated from all sides except the right wall where a copper wall is used to exchange heat between the water and PCM.

RT-35 (RUBITHERM), which is among the organic PCMs, is used in this study and its physical properties are listed in Table 1. Note that the PCM is initially at 300 K in the melting process and 323 K in the solidification process.

Table 1

Physical properties of RT 35 [8].

Property	Density (kg/m^3)	Heat of fusion (kJ/kg)	Specific heat (kJ/kg.K)	Thermal conductivity (W/m.K)	Viscosity (Pa.s)	Liquidus temperature (K)	Solidus temperature (K)	Thermal expansion coefficient (1/K)
values	815	170	2.0	0.2	0.023	309	302	0.0006

Note that for the composite PCM, the length of the heat storage unit extends based on the porosity of the copper foam due to having a constant volume of the PCM compared with the PCM only cases to have a reasonable comparison.

4. Numerical model and validation

The governing equations are solved using ANSYS-FLUENT. The equations are discretised with double precision solver using the SIMPLE algorithm with Presto scheme for pressure correction equation and QUICK scheme for the momentum and energy equations. The values of 0.3, 0.3, 1.0 and 0.5 are used as the under relaxation factors for the pressure, velocity, energy, and the liquid fraction, respectively. The convergence criteria for all the continuity, momentum and energy equations are set to 10^{-6}. Grid independency test is also performed on different grid sizes of 48000, 64000 and 80000 elements presented in Table 2 for the LHTES-w with A=0.3 and L=1.25. Table 2 presents the results of melting time and average temperature of the PCM after the meting process for different element numbers. The results show that the maximum difference in the melting time is less than 2% between using 64000 elements and 80000 elements with a time step of 0.2 s. Therefore, the grid with the size of 64000 elements is chosen as the best grid.

Table 2

Grid independency analysis

Number of elements	Melting time (s)	Average temperature (K)
48000	780	316.35
64000	812	316.66
80000	822	316.74

Different time step sizes of 0.05, 0.1 and 0.2 s for a constant grid size of 64000 cells for the LHTES-W system are studied and no change is seen in the variation of liquid fraction. The reason is that the velocity is low and the thermal front movement is similarly low, reflecting a low Peclet number and Courant number situation.

To validate the code, the numerical results of Liu et al. [33] are used for temperature comparison using a copper foam/PCM with the porosity of 95% and pore density of 10 PPI using RT-58. The geometry was first generated in the experimental work of Zhao et al. [2] which is a rectangular enclosure with a heat flux boundary condition from the bottom and free convection for the walls. Liu et al. [33] simulated the system using both thermal equilibrium and non-equilibrium models for the porous-PCM. The results of the temperature at the height of 8 mm from the bottom is presented here for the validation compared with the results of the thermal equilibrium model of Liu et al. [33] in Fig. 6 showing a good agreement.

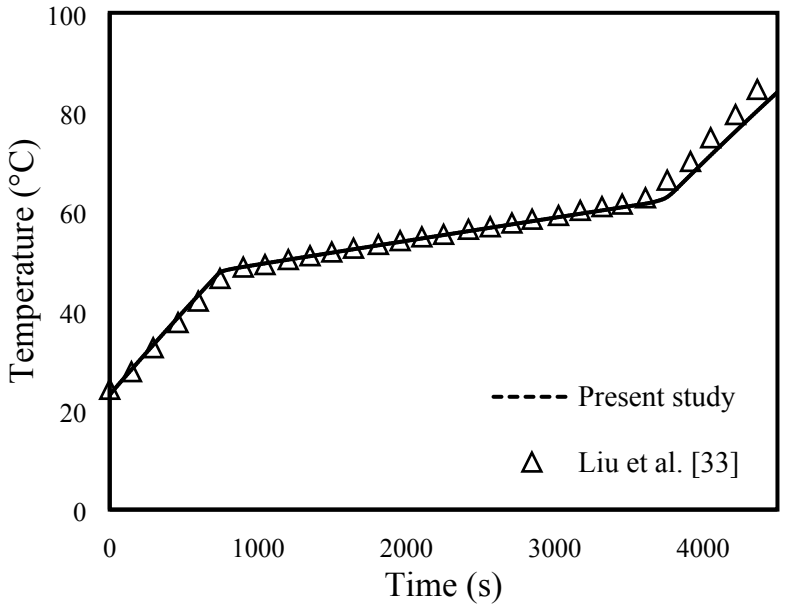

Fig. 2. The validation results of porous-PCM simulation compared with numerical studies of Liu et al. [33]

5. Results and discussion

In the following, for both melting and solidification sections, the results of the composite copper foam/PCM and PCM alone systems are presented for both the LHTES-W and LHTES-S systems. Then, for the composite PCM case, the effects of the wave amplitude, wavelength, pore size, porosity, inlet temperature and Reynolds number of the water are discussed. Note that the volume of the porous PCM LHS systems is increased according to the porosity of the copper foam due to considering constant volume and mass of the PCM in all the simulations to have a meaningful comparison of the results.

5.1. The Melting process

5.1.1. Composite copper foam/PCM vs. Pure PCM

Fig. 3 illustrates the temperature contours of the LHTES-W system with composite copper foam/PCM (on the top) and pure PCM (on the bottom) in the melting process. The temperature is transferred much quicker in the composite PCM system which shows the higher effect of adding porous structure than the natural convection. Heat transfer from water to the PCM

occurs by two mechanisms of conduction and convection. In the system with composite PCM, due to the higher conductivity of the copper foam compared with the pure PCM, the presence of the copper foam intensifies the rate of conduction heat transfer. However, from the point of view of convection heat transfer, the presence of copper foam suppresses the effect of natural convection due to making flow resistance in the movement of the fluid. At the beginning, when the amount of liquid PCM is low, heat transfer is mainly occurred by the conduction mechanism which is, therefore, higher in the case of composite PCM rather than the pure PCM.

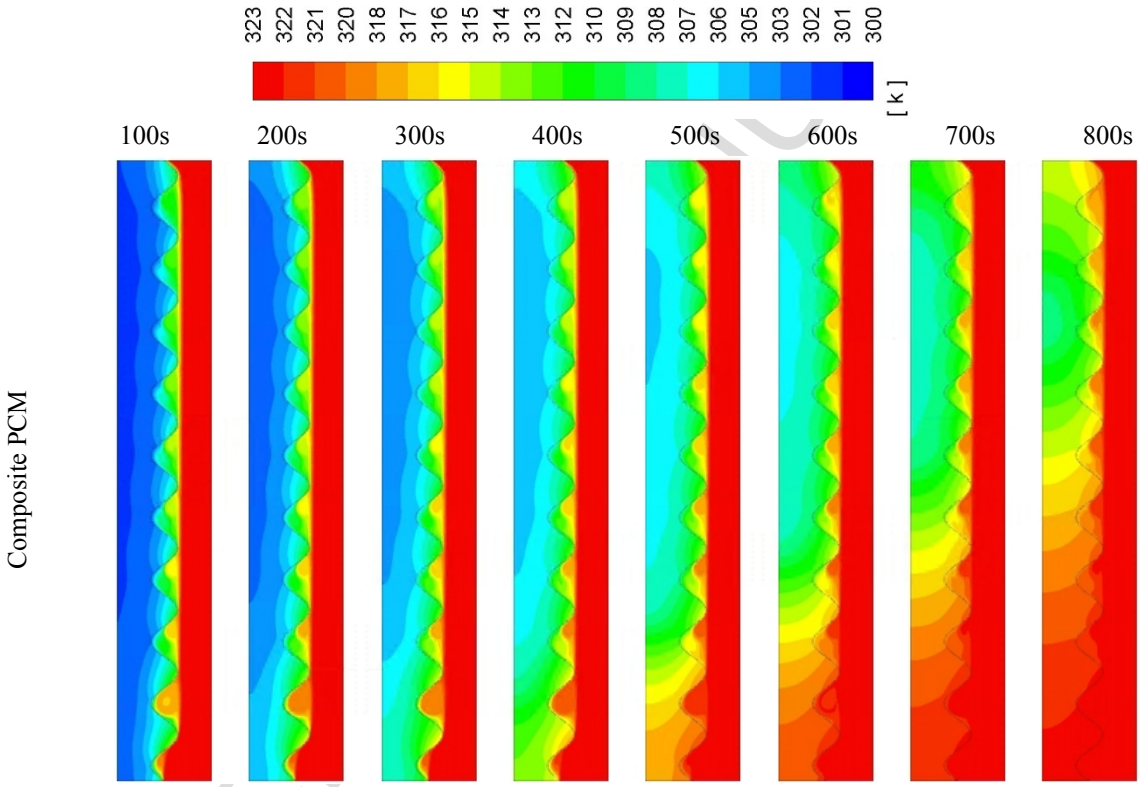

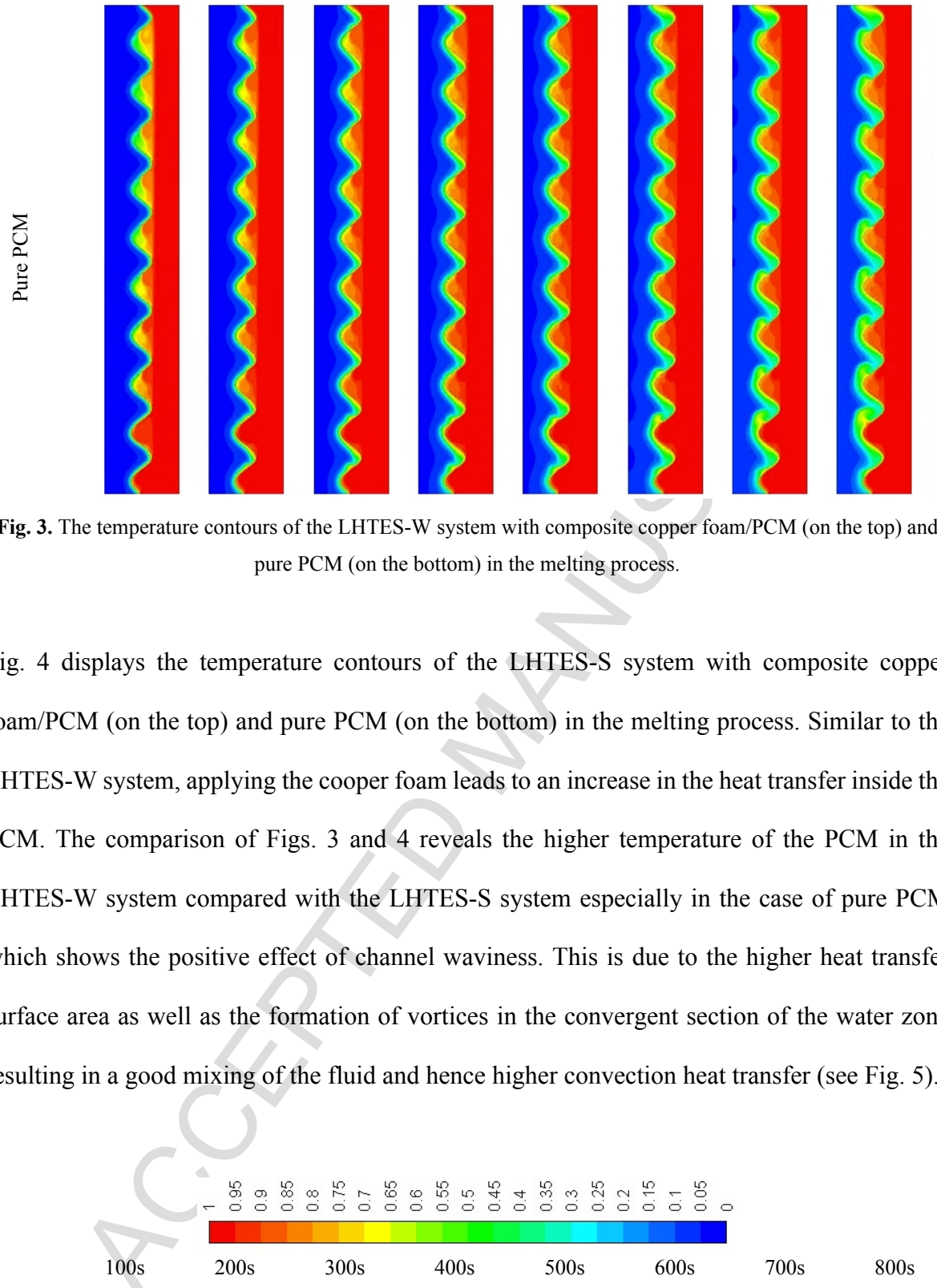

Fig. 3. The temperature contours of the LHTES-W system with composite copper foam/PCM (on the top) and pure PCM (on the bottom) in the melting process.

Fig. 4 displays the temperature contours of the LHTES-S system with composite copper foam/PCM (on the top) and pure PCM (on the bottom) in the melting process. Similar to the LHTES-W system, applying the cooper foam leads to an increase in the heat transfer inside the PCM. The comparison of Figs. 3 and 4 reveals the higher temperature of the PCM in the LHTES-W system compared with the LHTES-S system especially in the case of pure PCM which shows the positive effect of channel waviness. This is due to the higher heat transfer surface area as well as the formation of vortices in the convergent section of the water zone resulting in a good mixing of the fluid and hence higher convection heat transfer (see Fig. 5).

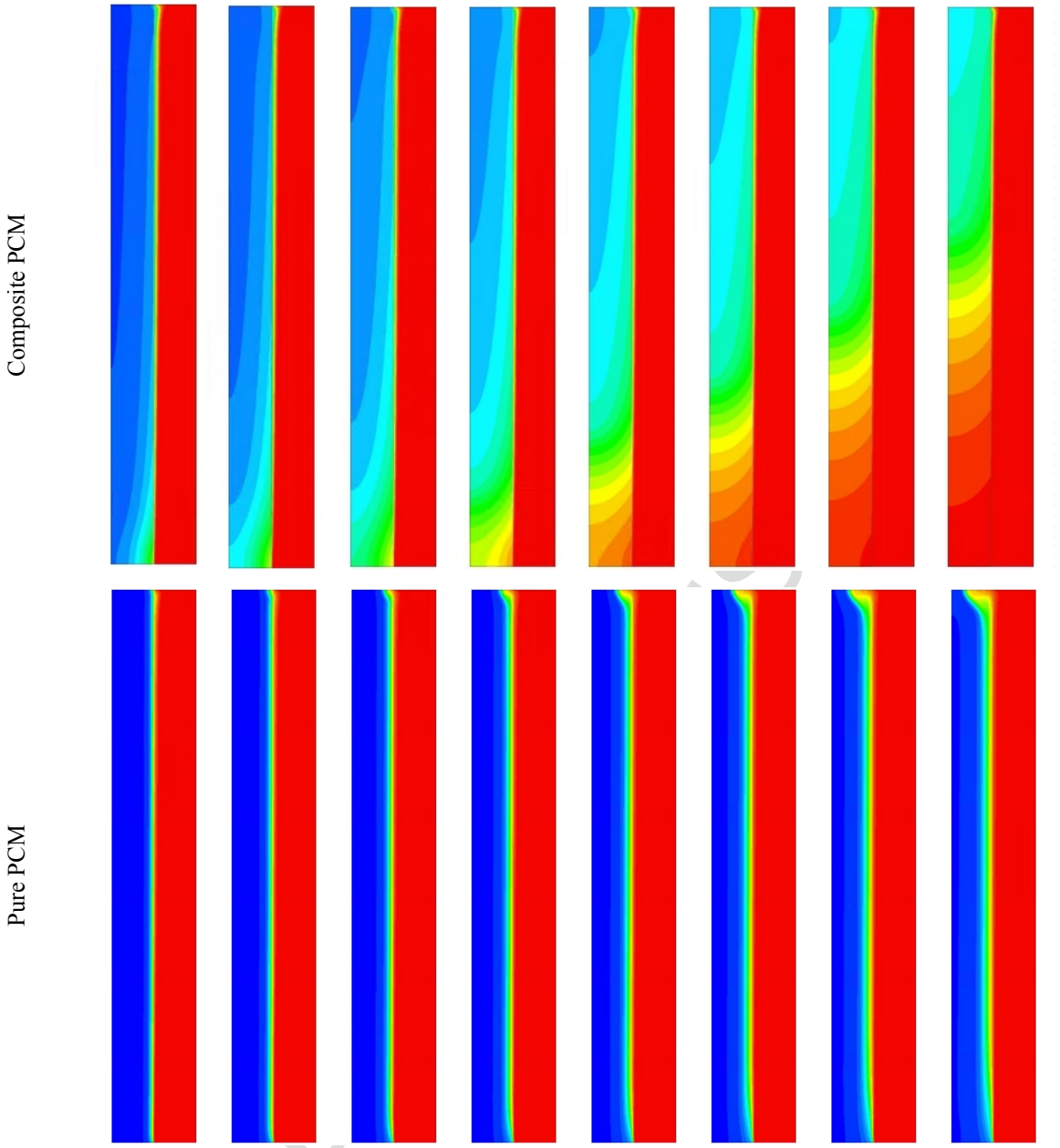

Fig. 4. The temperature contours of the LHTES-S system with composite copper foam/PCM (on the top) and pure PCM (on the bottom) in the melting process.

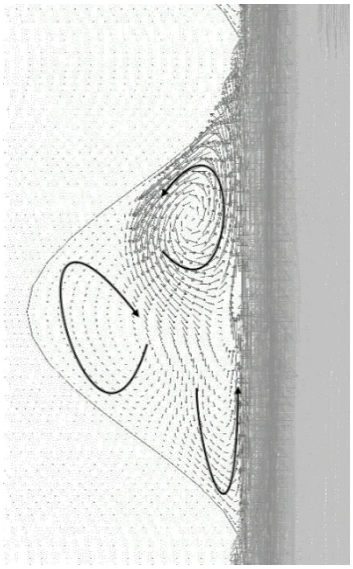

Fig. 5. Velocity vectors of the water at the time of 30 minutes for the LHTES-W system.

The variation of the average PCM temperature as a function of time for both the LHTES-W and LHTES-S systems is demonstrated in Fig. 6. The difference between the mean temperatures of the LHTES-W and LHTES-S systems containing composite PCM are small. This is due to the enhancement of heat transfer rate by the porous structure which suppress the effect of channel waviness. For the pure PCM case, the effect of channel waviness results in a higher temperature of the PCM at the same time compared with the LHTES-S system.

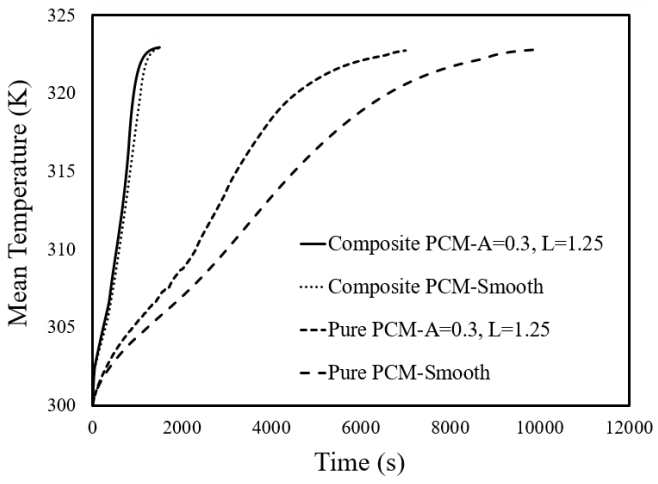

Fig. 6. Average PCM temperature as a function of time for the LHTES-W and LHTES-S systems using composite PCM and pure PCM in the melting process.

Fig. 7 depicts the contours of liquid fraction for the LHTES-W system with composite copper foam/PCM (on the top) and pure PCM (on the bottom) in the melting process. Due to the higher temperature of PCM in the case of composite PCM, the melting temperature is reached quicker and therefore higher values of the liquid fraction can be seen at an identical time compared with the pure PCM. In the case of composite PCM, all the PCM becomes liquid after 800s, while in the pure PCM case, just a thin layer near the mid-wall is melted and the rest is still in the solid state.

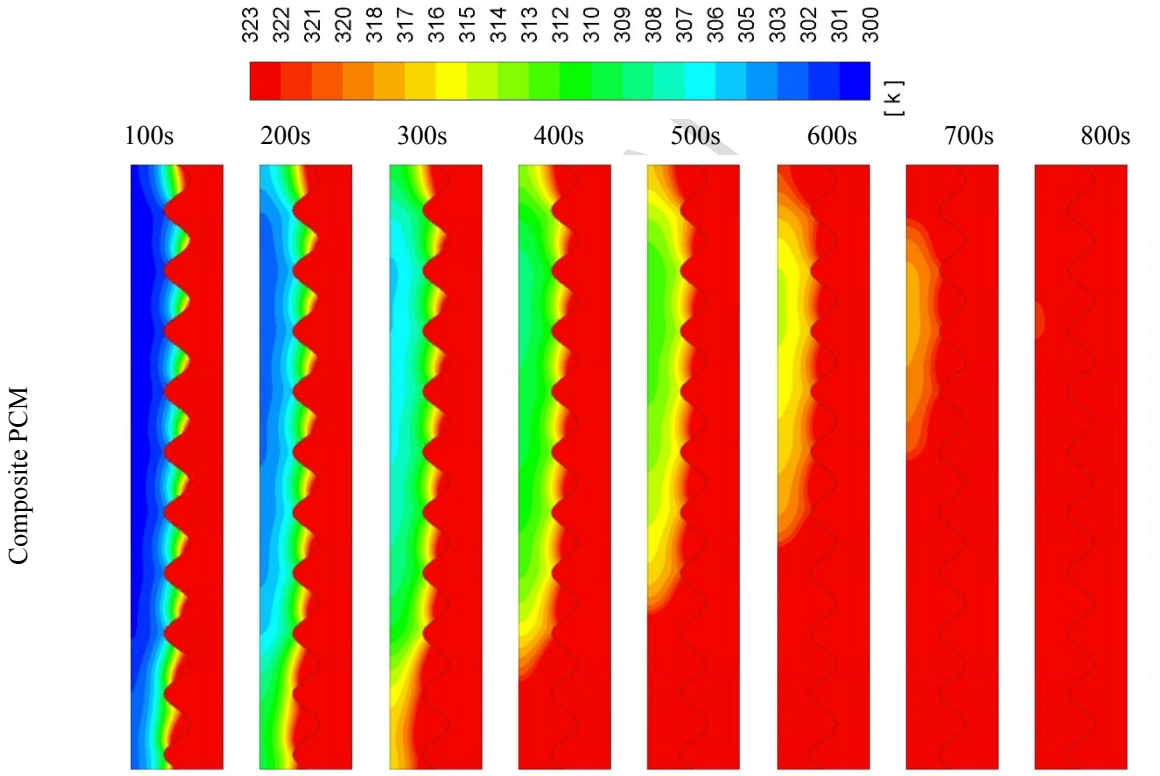

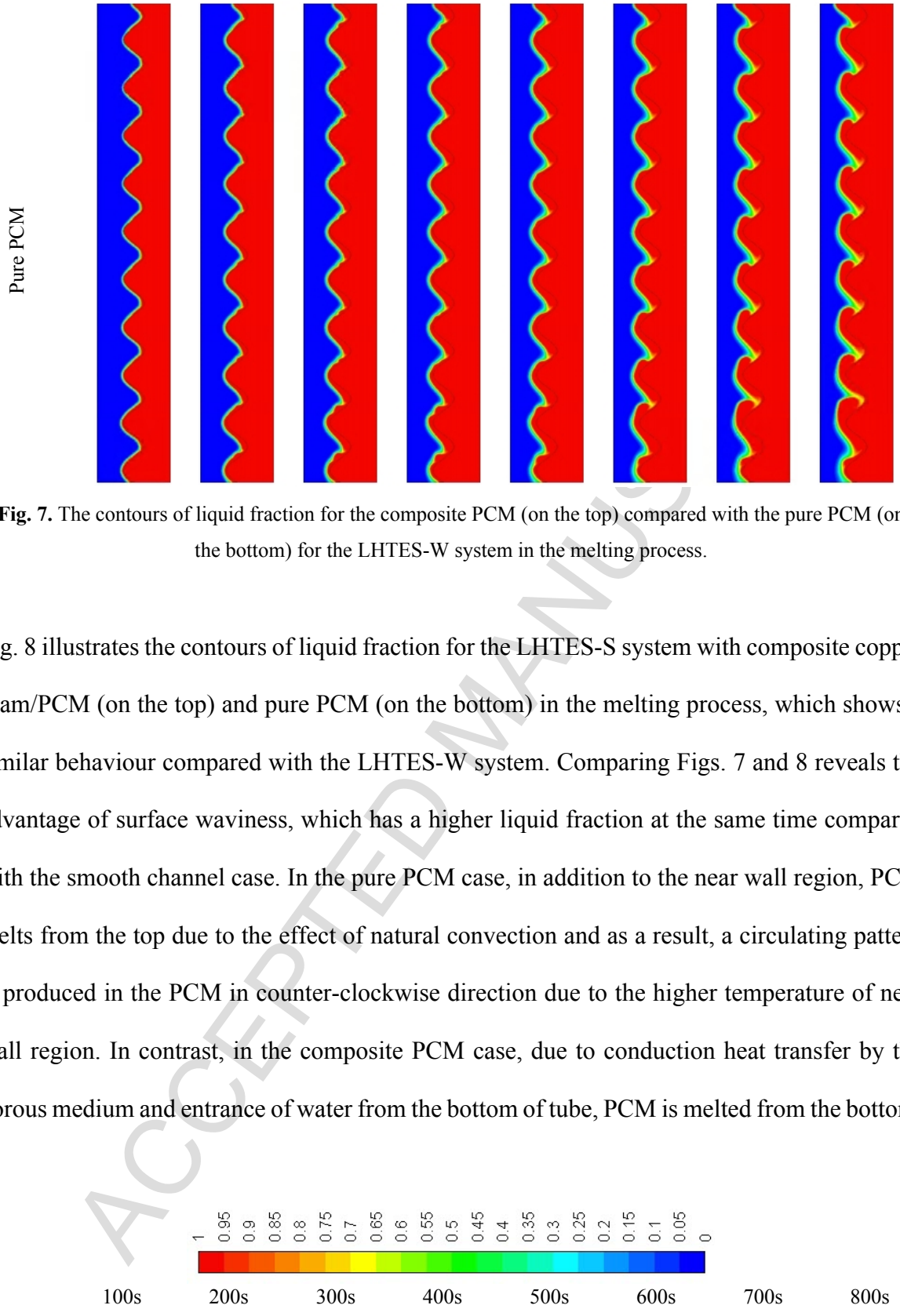

Fig. 7. The contours of liquid fraction for the composite PCM (on the top) compared with the pure PCM (on the bottom) for the LHTES-W system in the melting process.

Fig. 8 illustrates the contours of liquid fraction for the LHTES-S system with composite copper foam/PCM (on the top) and pure PCM (on the bottom) in the melting process, which shows a similar behaviour compared with the LHTES-W system. Comparing Figs. 7 and 8 reveals the advantage of surface waviness, which has a higher liquid fraction at the same time compared with the smooth channel case. In the pure PCM case, in addition to the near wall region, PCM melts from the top due to the effect of natural convection and as a result, a circulating pattern is produced in the PCM in counter-clockwise direction due to the higher temperature of near wall region. In contrast, in the composite PCM case, due to conduction heat transfer by the porous medium and entrance of water from the bottom of tube, PCM is melted from the bottom.

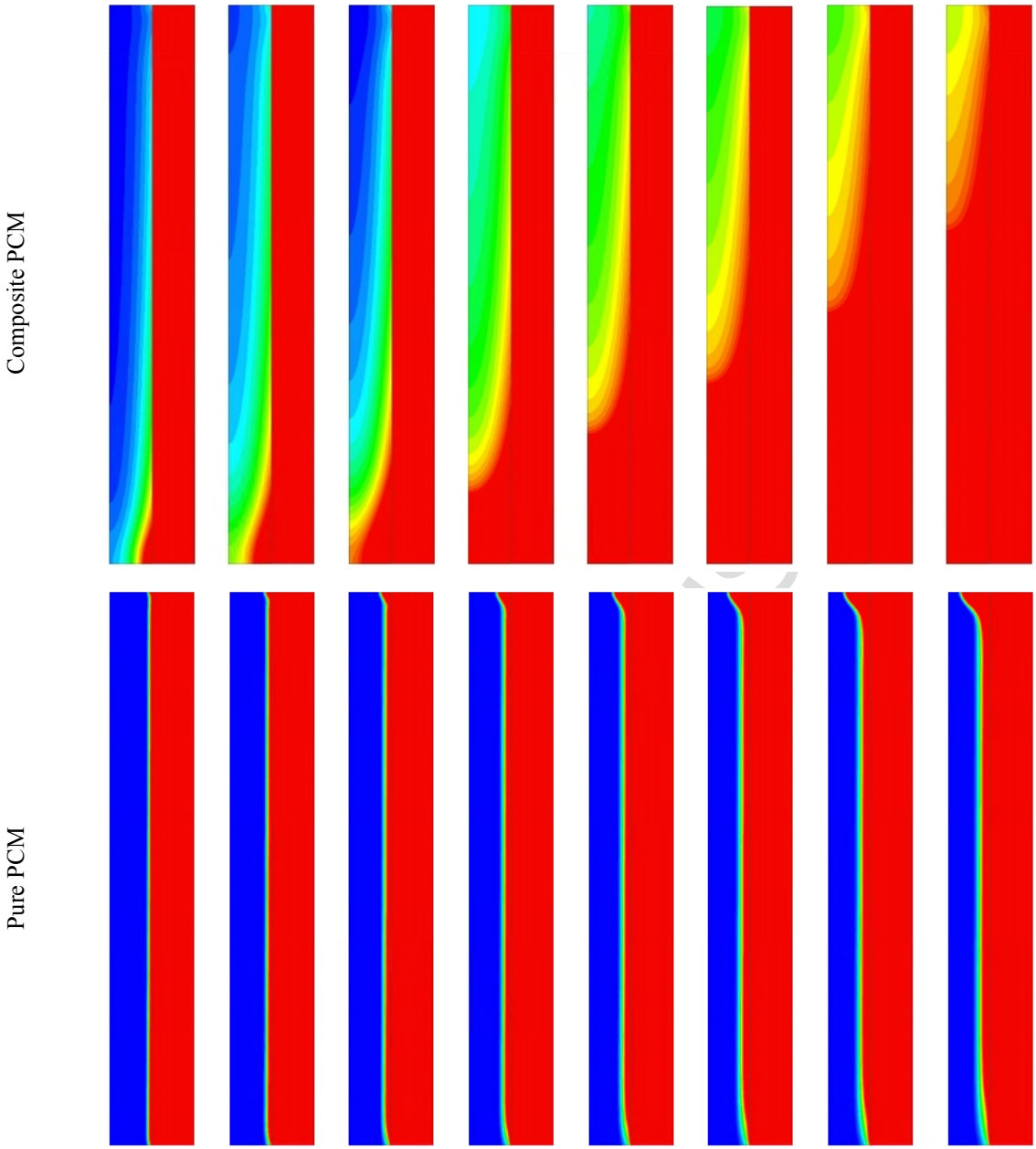

Fig. 8. The contours of liquid fraction for the composite PCM (on the top) compared with the pure PCM (on the bottom) for the LHTES-S system in the melting process.

The variation of the PCM liquid fraction as a function of time for both the LHTES-W and LHTES-S systems is shown in Fig. 9. It is seen that in the presence of the porous medium, the effect of channel waviness is suppressed. As mentioned before, this is due to the enhancement of heat transfer rate by the porous structure which suppress the effect of channel waviness.

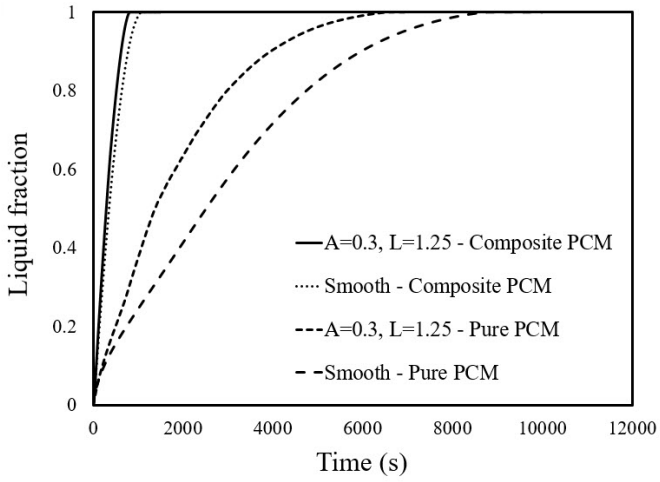

Fig. 9. PCM liquid fraction as a function of time for the LHTES-W and LHTES-S systems using composite PCM and pure PCM in the melting process.

Table 3 lists the characteristics of the LHTES-W and LHTES-S systems with composite PCM and pure PCM at $Re = 2000$ and $T_{in} = 323$ K in the melting process. The reported parameters include the melting time, liquid fraction at the minimum time, total amount of transferred heat from the PCM to the water (Q), average rate of transferred heat ($\dot{Q}$), pressure drop (ΔP), and pumping power ($\dot{W}$). The pumping power is calculated by the product of volume flow rate of water and pressure drop. Note that for the calculation of Q and $\dot{Q}$, the rate of transferred heat through the copper wall between the PCM and water are determined from the FLUENT report. For both systems, the melting time reduces by almost 88.7% through using the porous copper foam inside the PCM. For the LHTES-W system, at the time of 812 s (i.e., minimum time) when all the PCM is melted, the liquid fraction of the PCM alone system is 0.29 which means that 71% of stored heat in the PCM is still unused. Comparing the results of pressure drop and pumping power reveals that the channel waviness has a negligible effect on the pressure drop and therefore, the pumping power does not increase by employing the channel waviness.

Table 3

The characteristics of the LHTES-W and LHTES-S systems with composite PCM and pure PCM at $Re = 2000$ and $T_{in} = 323$ K in the melting process.

PCM type	Case	Melting time (s)	λ	Q (kJ)	$\dot{Q}$ (W)	ΔP (Pa)	$\dot{W}$ (mW)
Composite PCM	LHTES-W	812	1	156.5	192.7	356.39	17.87
	LHTES-S	1069	0.92	174.8	163.5	355.65	17.84
Pure PCM	LHTES-W	7176	0.29	174.2	24.3	356.39	17.87
	LHTES-S	9425	0.25	175.5	18.6	355.65	17.84

5.1.2. Effect of waviness characteristics

Fig. 10 displays the PCM liquid fraction for different channel wave amplitudes for the LHTES-W system with composite PCM at $L = 1.25$. Due to the presence of the porous medium and the role of copper foam in the heat transfer enhancement, the difference between the melting times of various wave amplitudes is low. Furthermore, in general, increasing the amplitude results in a lower melting time due to a higher heat transfer surface area and improved mixing of water as well as the melted PCM. Note that $A = 0$ means the smooth channel.

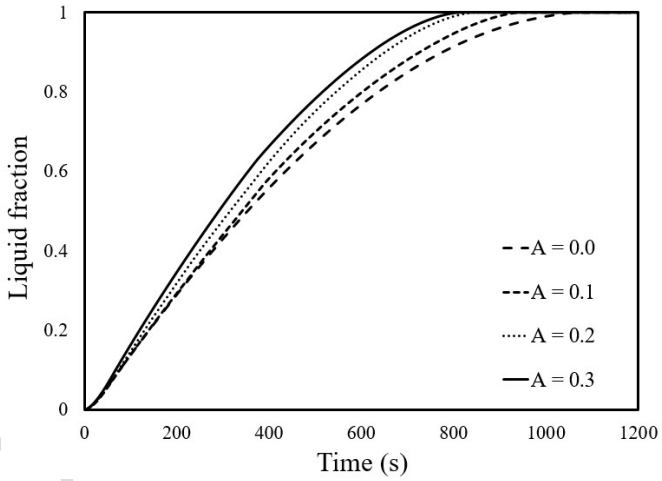

Fig. 10. The effect of wave amplitude on the liquid fraction for the LHTES-W system with composite PCM in the melting process.

Fig. 11 displays the variation of the liquid fraction for different wavelengths of the channel with $A = 0.3$. Similar to the wave amplitude, due to the presence of the porous medium, the difference between the melting times of LHTES-W system with various wavelengths is low.

Furthermore, Fig. 11 depicts that increasing the wavelength of the channel results in a higher melting time.

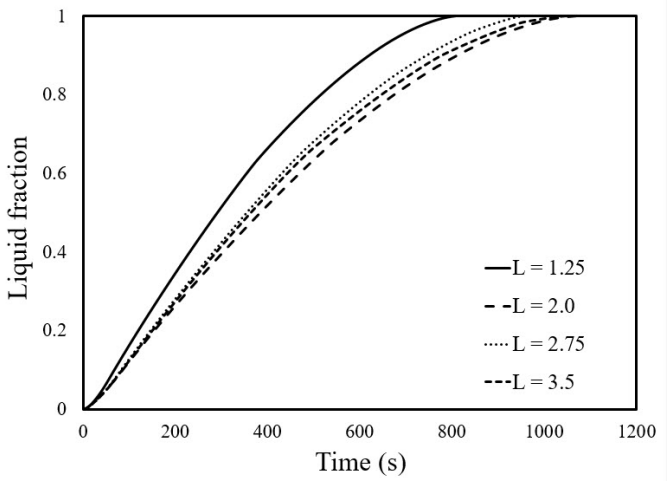

Fig. 11. The effect of wavelength on the liquid fraction for the LHTES-W system with composite PCM in the melting process.

Table 4 schematized the melting time, the total amount of transferred heat (Q), the average rate of transferred heat ($\dot{Q}$), TES rate (p), TEs density (q) and TES rate density (w)for different systems at $Re = 2000$ and $T_{in} = 323$ K. As mentioned, for the calculation of p, just the latent heat of fusion in considered, while, for the $\dot{Q}$, both the sensible and latent heat are considered and therefore p is always smaller than $\dot{Q}$. However, as shown in Table 4, the difference between p and $\dot{Q}$ is not high since the LHTES acts based on the latent heat of fusion rather than sensible heat. Furthermore, due to having a constant mass for the PCM and the foam, q is similar for different cases. For the best case, the melting time can be saved by almost 24% and the average rate of heat transfer enhances by almost 17.9% compared with the LHTES-S system containing composite PCM.

Table 4

The characteristics of the studied LHTES-W systems with composite PCM at Re = 2000 and T_{in} = 323 K in the melting process.

Case	A	L	Melting time (s)	Q (kJ)	$\dot{Q}$ (W)	p (W)	q (kJ)	w (W)
Smooth channels	-	-	1069	174.8	163.5	116.0	107.6	100.7
Sinusoidal wavy channels	0.1	1.25	942	167.9	178.2	131.7	107.6	114.2
	0.2	1.25	845	160.9	190.5	146.8	107.6	127.3
	0.3	**1.25**	**812**	**156.6**	**192.8**	**152.8**	**107.6**	**132.5**
	0.3	2	1077	155.6	144.5	115.2	107.6	99.9
	0.3	2.75	964	147.4	152.9	128.7	107.6	111.6
	0.3	3.5	1051	147.8	140.7	118.0	107.6	102.4

5.1.3. Effect of porous structure characteristics

The characteristics of the porous medium are defined by three parameters including the porosity, pore density, and ligament diameter and by knowing two of these parameters, the other one can be calculated. The variation of the liquid fraction for different pore densities is displayed in Fig. 12 for the porosity of 95%. A higher value of pore density (higher PPI) means a smaller size of a pore results in a higher surface area per volume and therefore, a higher rate of heat transfer between the PCM and the copper foam. On the other hand, it suppresses the effect of natural convection due to the high flow resistance in the fluid flow direction [33]. Therefore, the effect of pore size is related to the geometry, initial conditions and material of the PCM and porous medium. As shown, in general, the pore size has a negligible effect on the variation of liquid fraction. The liquid fraction increases by increasing the pore size from 10 PPI to 30 PPI and then is almost not changed compared with the 50 PPI case.

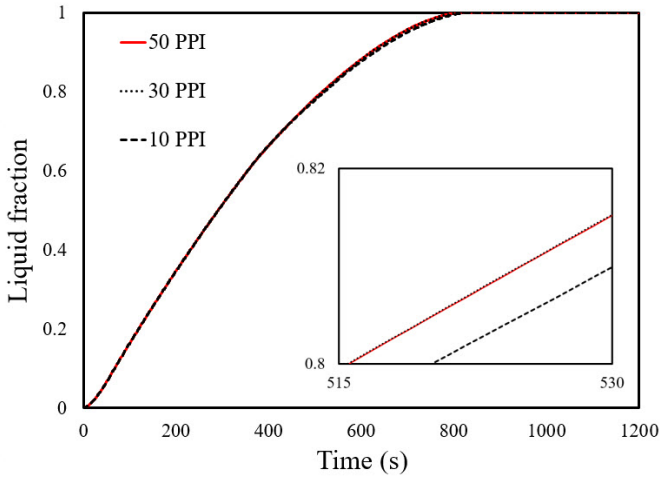

Fig. 12. The effect of pore size on the liquid fraction for the LHTES-W system with composite PCM in the melting process.

The variation of the liquid fraction for different porosity of copper foam is displayed in Fig. 13 for the pore size of 30 PPI. As expected, by increasing the porosity of the copper foam and therefore, reducing the amount of copper inside the domain, the PCM melts in a longer time due to a lower rate of heat transfer. Even for the porosity of 98% in the sinusoidal double-pipe heat storage unit, the melting time reduces by 85% compared with the pure PCM case with the same geometry.

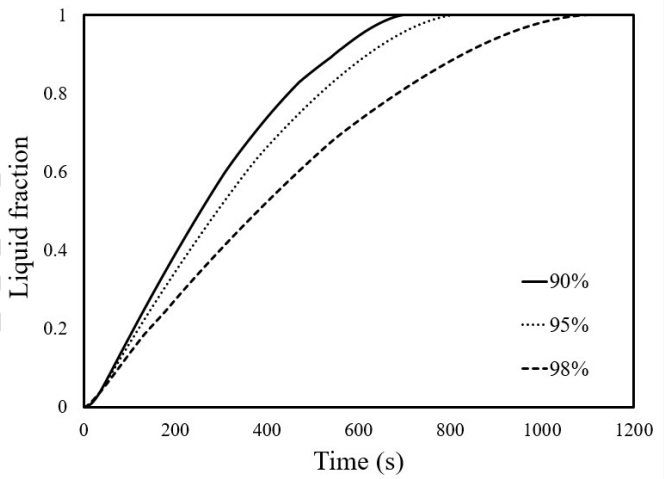

Fig. 13. The effect of foam porosity on the liquid fraction of the composite PCM inside the LHTES-W system in the melting process.

5.1.4. Effect of HTF characteristics

Fig. 14 displays the effect of water inlet temperature in the melting process on the liquid fraction of PCM inside the LHTES-W system with composite PCM at $A = 0.3$ and $L = 1.25$ with the porosity of 95% and pore size of 30 PPI. It is clear that by increasing the water inlet temperature, more heat is transferred to the PCM and consequently, lower melting time is achieved. By increasing the inlet temperature from 318 to 323 K and 318 to 328 K, the melting time increases by 27.2% and 40.1%, respectively.

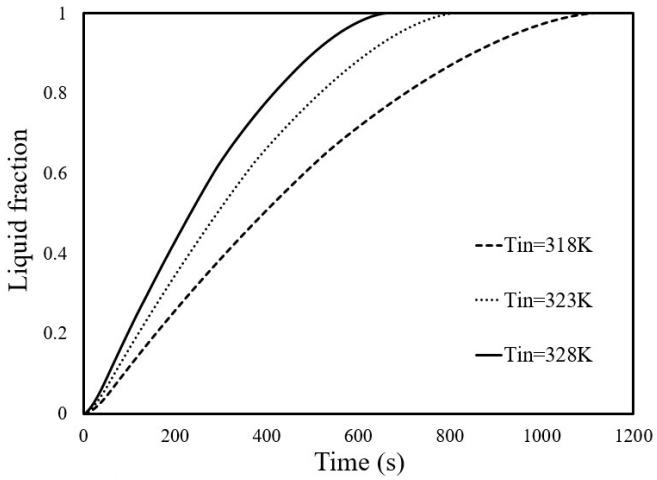

Fig. 14. The effect of inlet water temperature on the liquid fraction of the composite PCM inside the LHTES-W system in the melting process.

Fig. 15 demonstrates the effect of Reynolds number in the melting process on the liquid fraction of the composite PCM inside the LHTES-W system at $A = 0.3$ and $L = 1.25$. As shown, for a higher Reynolds number, a higher liquid fraction is achieved at an identical time and the melting time reduces with increasing the Reynolds number. This can be attributed to the fact that increasing the Reynolds number leads to the improved mixing of water and thereby, a higher heat transfer to the PCM container.

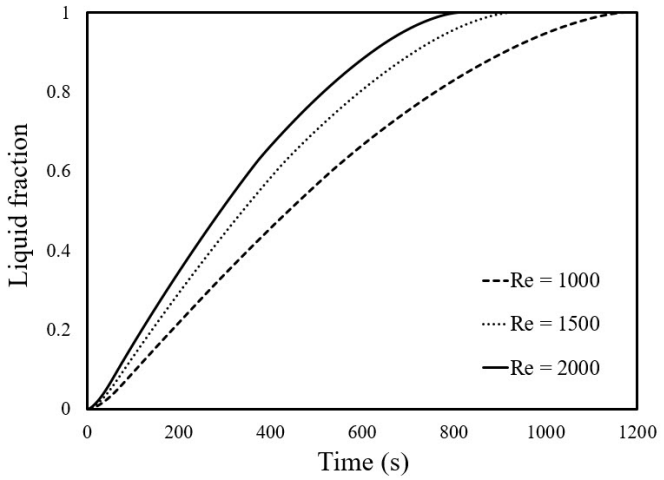

Fig. 15. The effect of water Reynolds number on the liquid fraction of the composite PCM inside the LHTES-W system in the melting process.

To better understand the effect of Reynolds number, Fig. 16 illustrates the generated vortices at the Reynolds numbers of 1000 and 2000. As shown, for the Reynolds number of 2000, more vortices form which causes higher mixing of the high-temperature water in the fluid zone results in a higher rate of heat transfer.

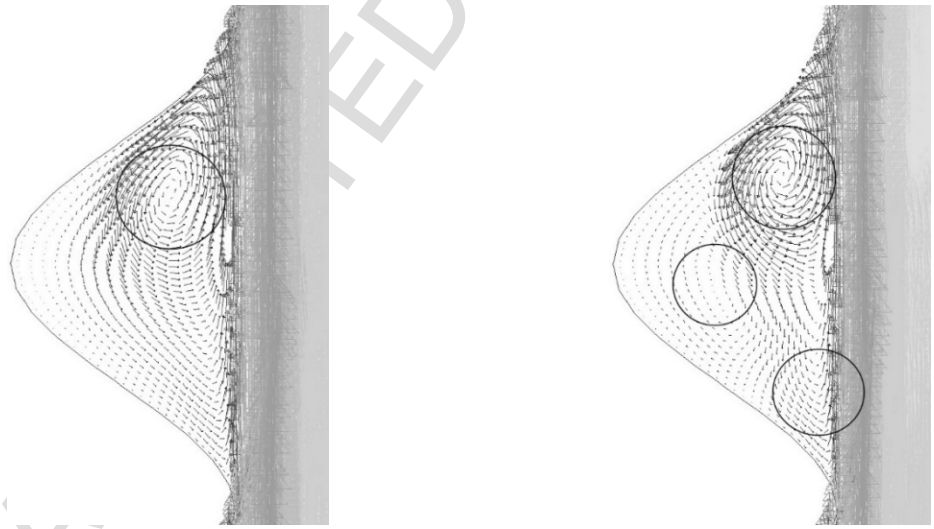

Re=1000 Re=2000

Fig. 16. Velocity vectors of the water for the LHTES-W system for different Reynolds numbers.

5.2. The Solidification process

5.2.1. Composite copper foam/PCM vs. pure PCM

Fig. 17 illustrates the temperature contours of the LHTES-W system with composite copper foam/PCM (on the top) and pure PCM (on the bottom) in the solidification process. Similar to the melting process, due to the presence of a copper foam, the rate of heat transfer enhances significantly. Therefore, temperature reduction happens quicker in the composite PCM case which causes the composite PCM to solidify in a less time compared with the pure PCM case.

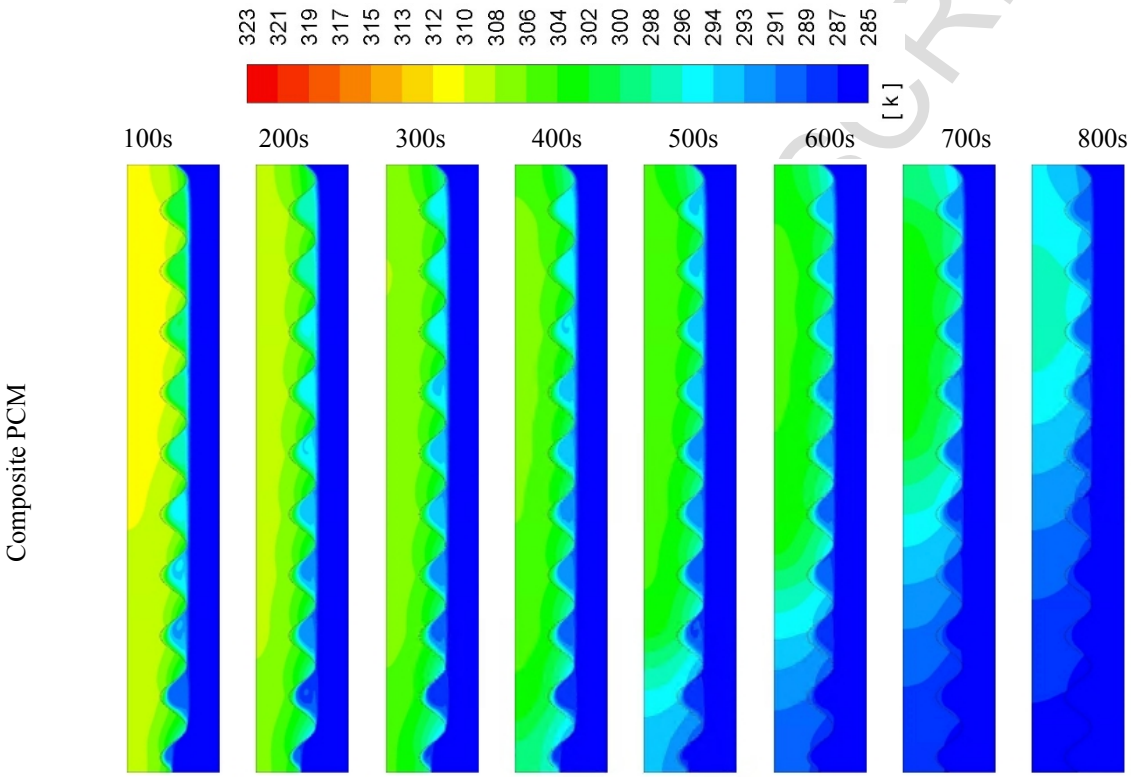

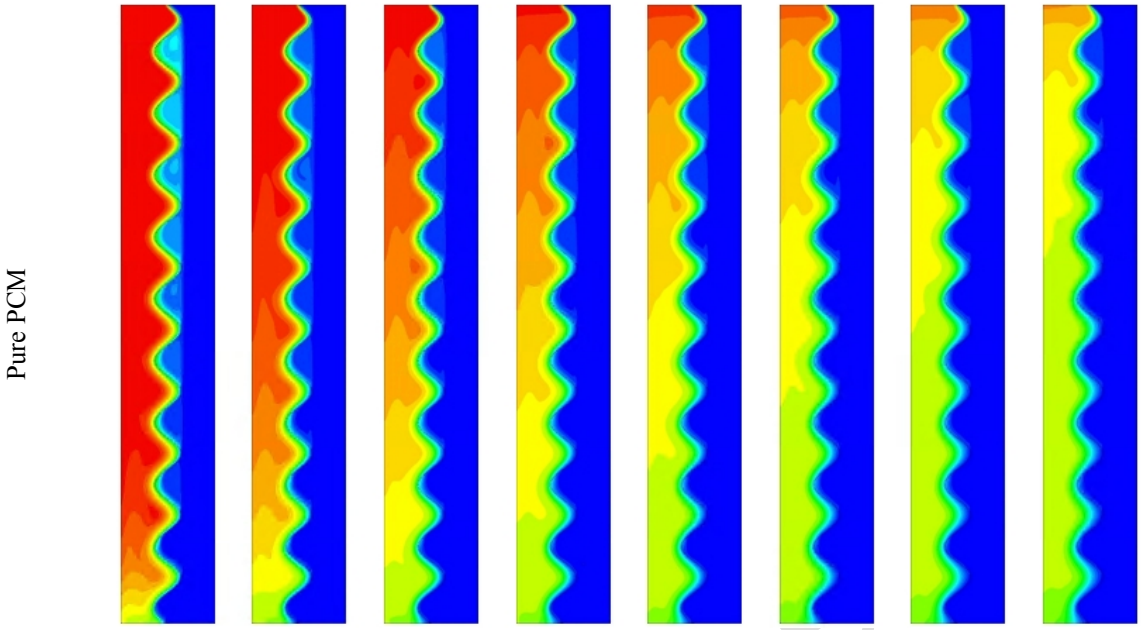

Fig. 17. The temperature contours of the LHTES-W system with composite copper foam/PCM (on the top) and pure PCM (on the bottom) in the solidification process.

Fig. 18 demonstrates the temperature contours of the LHTES-S system with composite copper foam/PCM (on the top) and pure PCM (on the bottom) in the solidification process. Similar trends can be seen in the comparison of composite PCM with pure PCM. The effect of waviness in the presence of porous structure shown in Figs. 17 and 18 reveals the advantage of channel waviness in the storage unit. Due to the higher heat transfer surface area and generated vortices in the water zone, larger areas with lower temperature can be seen in the LHTES-W system.

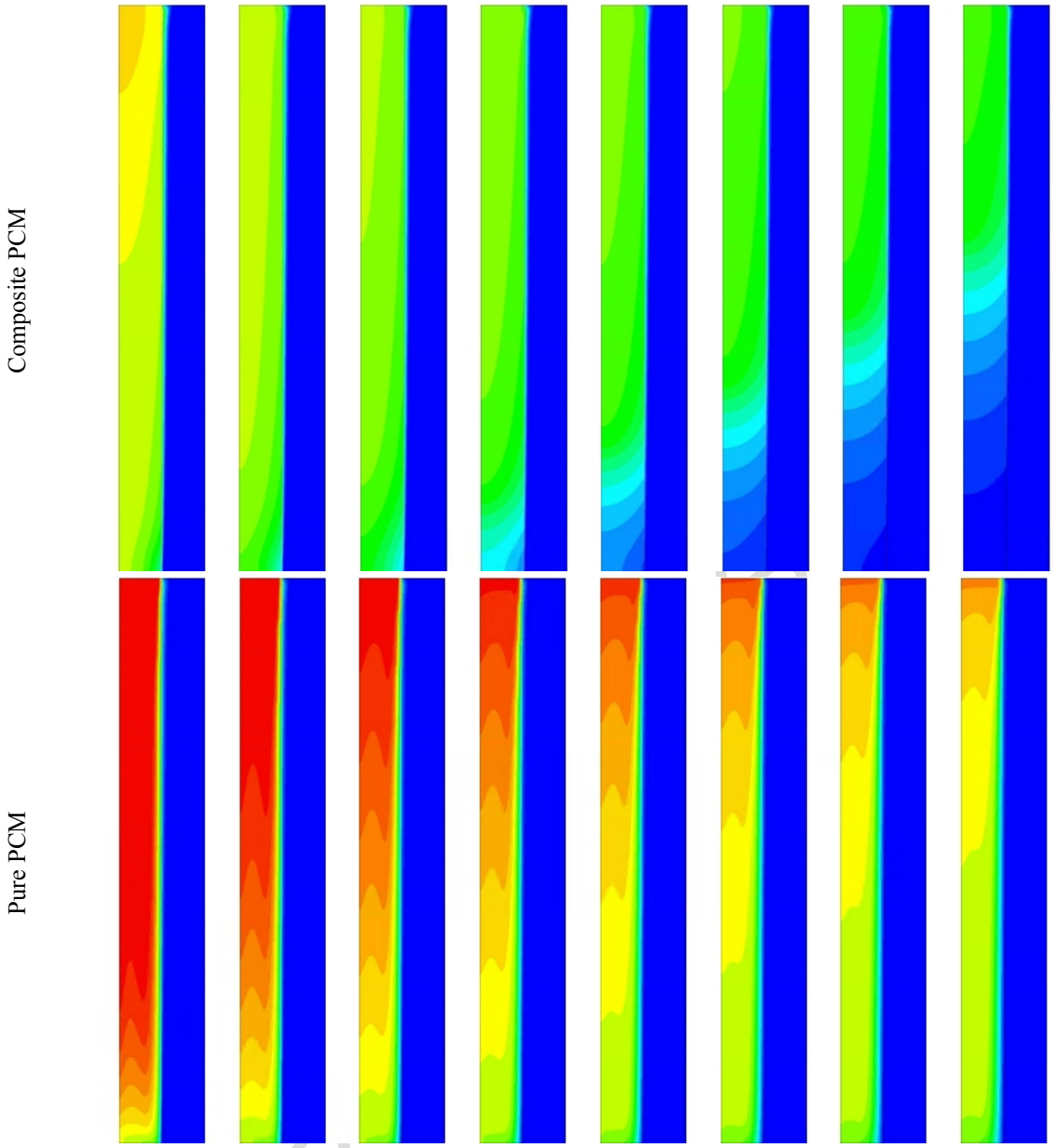

Fig. 18. The temperature contours of the LHTES-S system with composite copper foam/PCM (on the top) and pure PCM (on the bottom) in the solidification process.

The variation of the average PCM temperature as a function of time for both the LHTES-W and LHTES-S systems is demonstrated in Fig. 19. The difference between the mean temperatures of the LHTES-W and LHTES-S systems containing composite PCM are small. This is because of the enhancement of heat transfer rate by the porous foam. For the pure PCM case, the effect of channel waviness results in a lower temperature of the PCM at the same time compared to the LHTES-S system that reveals the advantageous effect of waviness alone.

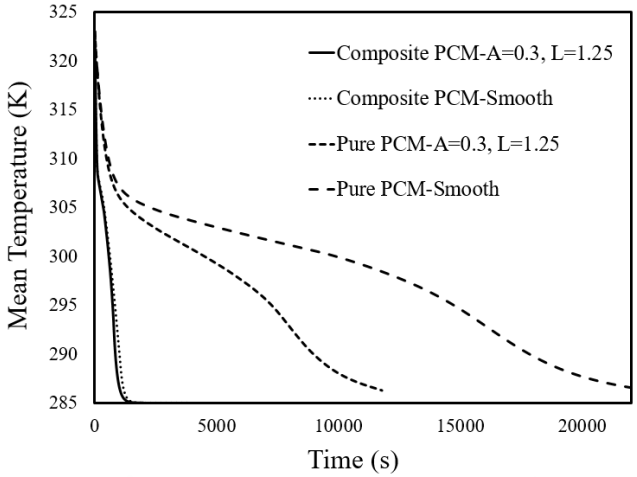

Fig. 19. Average PCM temperature as a function of time for the LHTES-W and LHTES-S systems using composite PCM and pure PCM in the solidification process.

Fig. 20 illustrates the contours of liquid fraction for the LHTES-W system with composite copper foam/PCM (on the top) and pure PCM (on the bottom) in the solidification process. Due to a lower temperature of PCM in the case of composite PCM, the solidification temperature is reached quicker and therefore, higher values of the liquid fraction can be achieved. After 800 s, all the PCM solidifies in the case of composite PCM while for the pure PCM case, just a thin layer near the mid-wall solidifies and the rest is still in the liquid state.

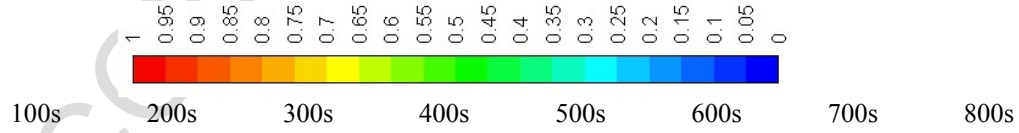

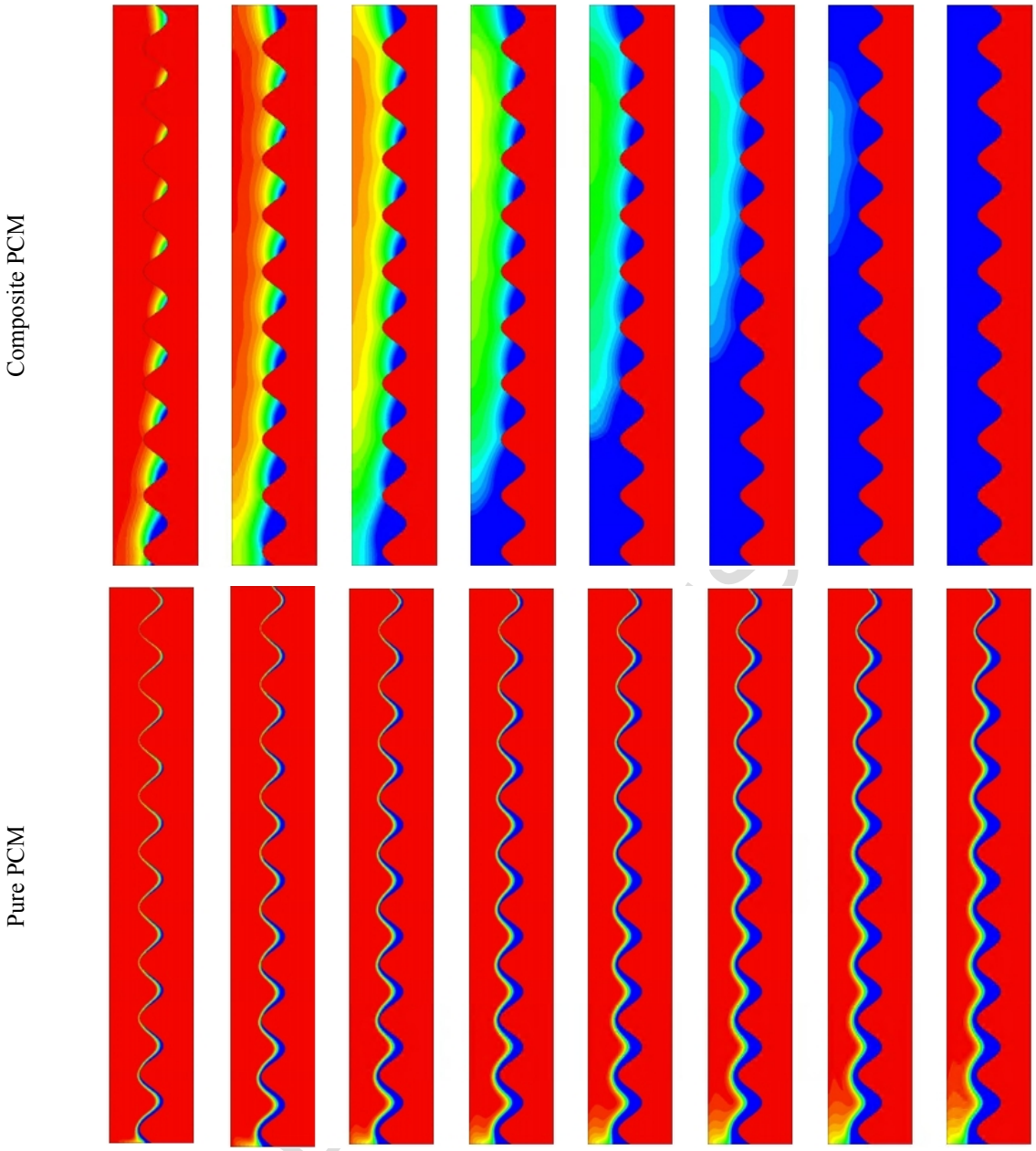

Fig. 20. The contours of liquid fraction for the composite PCM (on the top) compared with the pure PCM (on the bottom) for the LHTES-W system in the solidification process.

Fig. 21 displays the contours of liquid fraction for the LHTES-S system with composite copper foam/PCM (on the top) and pure PCM (on the bottom) in the solidification process, which shows a similar behaviour compared with the LHTES-W system. Channel waviness provides an enhancement of heat transfer rate, especially for the pure PCM case. As mentioned, the reason is that in the composite PCM case, the heat transfer from the PCM to the water occurs mainly through the porous structure. However, in the pure PCM case, the heat is transferred by

the PCM inside the domain and then distributed by the natural convection. Therefore, the sinusoidal wavy channels have enough time to improve the heat transfer characteristics.

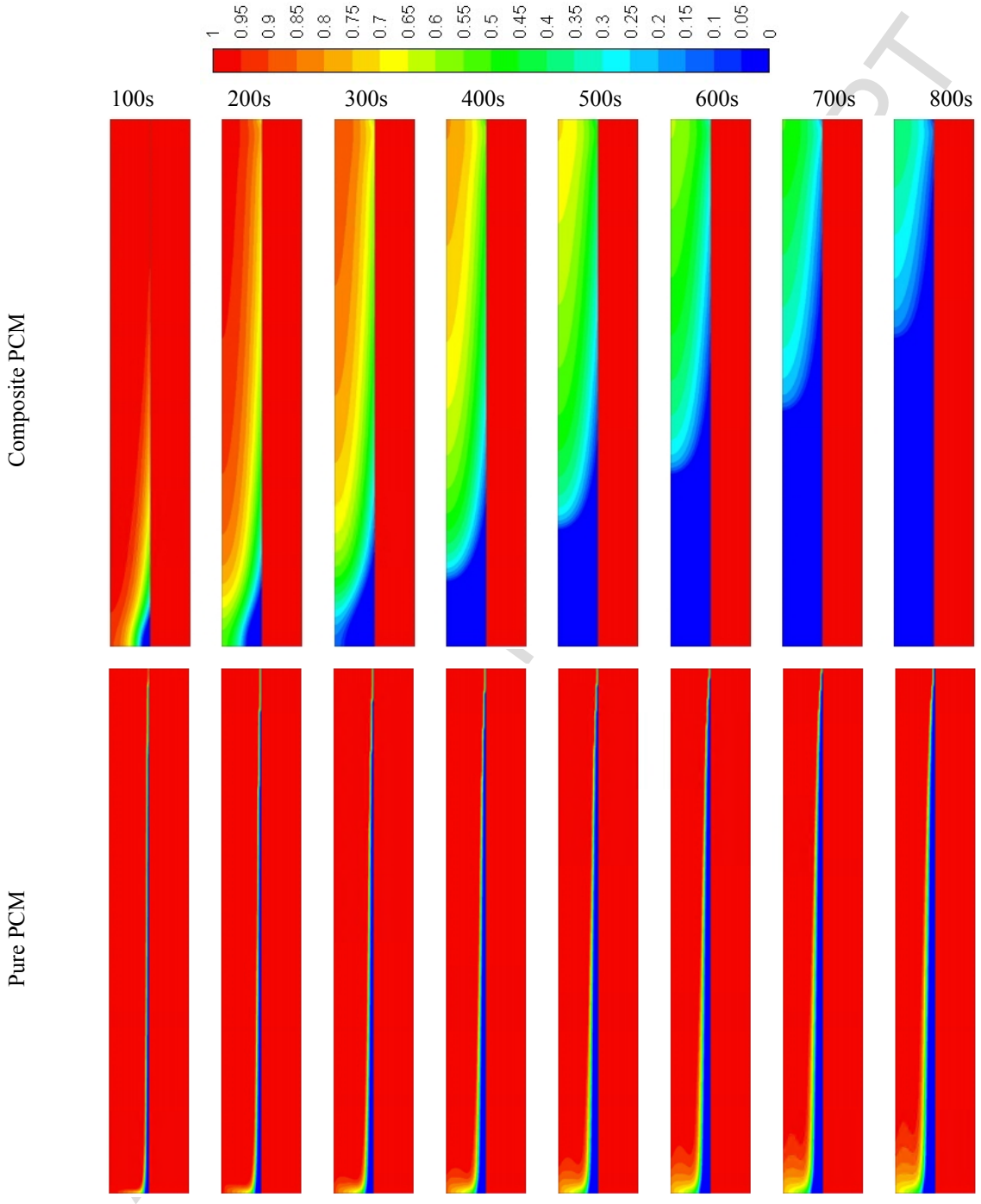

Fig. 21. The contours of liquid fraction for the composite PCM (on the top) compared with the pure PCM (on the bottom) for the LHTES-S system in the solidification process.

The variation of the PCM Liquid fraction as a function of time for both the LHTES-W and LHTES-S systems is depicted in Fig. 22. The melting time is reduced by significantly for the systems with composite PCM compared with the pure PCM systems due to the presence of a porous structure in the domain.

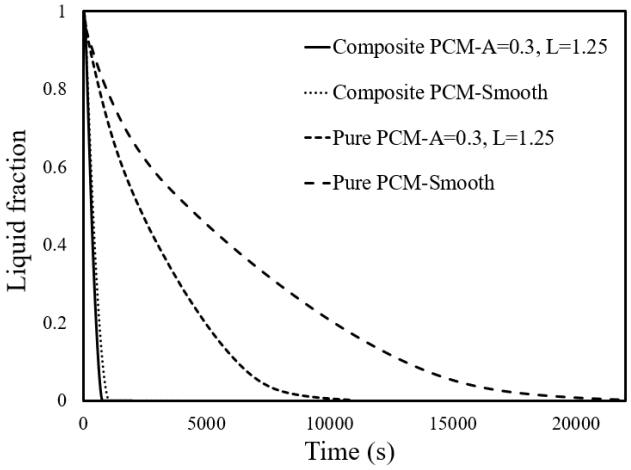

Fig. 22. PCM liquid fraction as a function of time for the LHTES-W and LHTES-S systems using composite PCM and pure PCM in the solidification process.

Table 5 reports the characteristics of the LHTES-W and LHTES-S systems with composite PCM and pure PCM at $Re = 2000$ and $T_{in} = 323$ K in the solidification process. For the LHTES-W system, the solidification time reduces by 93.3% by using the porous copper foam inside the PCM, while it is 95.5% for the LHTES-S system. For the LHTES-W system, at the time of 776 s when all the PCM melts, the liquid fraction of the PCM alone system is 0.78 which means that just 22% of the stored heat in the PCM is released to the water. Comparing the results of pressure drop and pumping power, similar to the melting process, reveals that the channel waviness has a negligible effect on the pressure drop and the pumping power.

Table 5

The characteristics of the LHTES-W and LHTES-S systems with composite PCM and pure PCM at $Re = 2000$ and $T_{in} = 323$ K in the solidification process.

PCM type	Case	Melting time (s)	λ	Q (kJ)	$\dot{Q}$ (W)	ΔP (Pa)	$\dot{W}$ (mW)
Composite PCM	LHTES-W	776	0	183.3	236.2	356.77	17.87
	LHTES-S	1043	0.1	197.9	189.7	356.11	17.84
Pure PCM	LHTES-W	11659	0.78	196.8	16.9	356.77	17.87
	LHTES-S	23305	0.79	292.2	12.5	356.11	17.84

5.2.2. Effect of channel waviness characteristics

Fig. 23 displays the variation of the liquid fraction for different wave amplitudes of the channel for the LHTES-W system with composite PCM at $L = 1.25$. Increasing the amplitude of the wave channel results in a lower solidification time due to the higher heat transfer surface area and improved mixing of water as well as the melted PCM. However, due to the presence of the porous medium and the main role of copper foam in the heat transfer enhancement, the difference between the solidification times for various wave amplitudes is small.

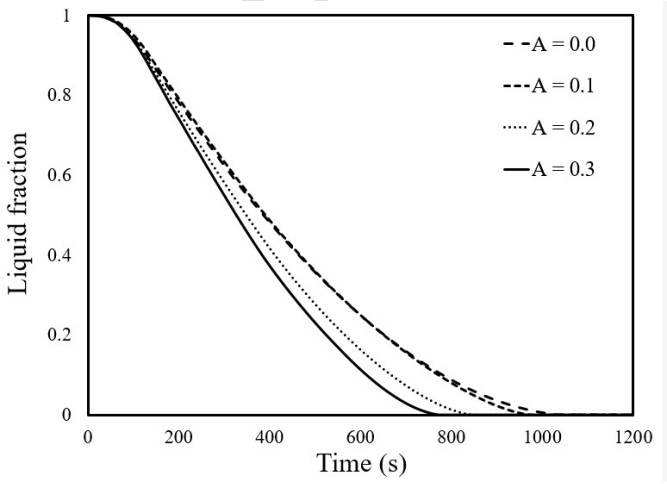

Fig. 23. The effect of wave amplitude on the liquid fraction for the LHTES-W system with composite PCM in the solidification process.

Fig. 24 displays the variation of the liquid fraction for different wavelengths of the channel in the composite PCM heat storage unit at $A = 0.3$. Increasing the amplitude of the wavy channel

results in a higher solidification time. However, similar to the wave amplitude, due to the presence of the porous medium, the difference between the solidification times for various wavelengths is low.

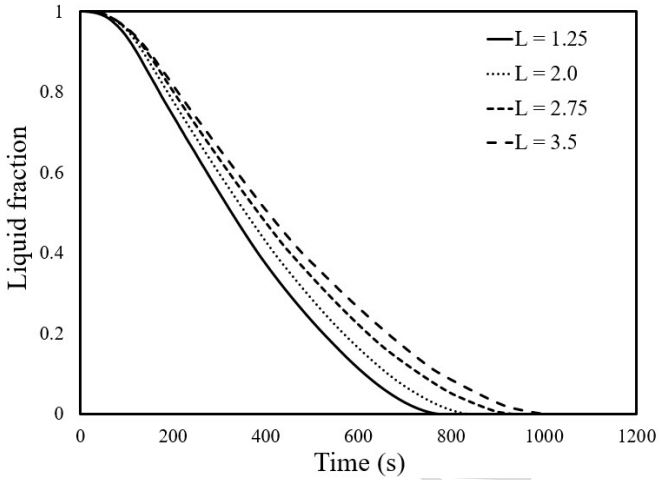

Fig. 24. The effect of wavelength on the liquid fraction for the LHTES-W system with composite PCM in the solidification process.

Table 6 lists the solidification time, Q, $\dot{Q}$, p, q and w for different LHTES units for the Reynolds number of 2000 and inlet water temperature of 285K. For the best case (A=0.3 and L=1.25), the solidification time reduces by almost 25.6% compared with the composite PCM LHTES system with smooth channels. Furthermore, the average rate of heat transfer enhances by almost 24.5% compared with the smooth channel system. Note that in the solidification process compared with melting, due to larger difference between the initial temperature (323K) and the liquidus temperature (302K), the difference between $\dot{Q}$ and p is higher.

Table 6

The characteristics of the studied LHTES-W systems with composite PCM at Re = 2000 and T_{in} = 323 K in the solidification process.

Case	A	L	solidification time (s)	Q (kJ)	$\dot{Q}$ (W)	p (W)	q (kJ)	w (W)
Smooth channels	-	-	1043	197.9	189.7	118.9	107.6	103.2
Sinusoidal wavy channels	0.1	1.25	977	192.7	197.2	127.0	107.6	110.1
	0.2	1.25	849	191	225	146.1	107.6	126.7
	0.3	**1.25**	**776**	**183.3**	**236.2**	**159.9**	**107.6**	**138.7**
	0.3	2	840	177.2	210.9	147.7	107.6	128.1
	0.3	2.75	937	176.2	188.1	132.4	107.6	114.8
	0.3	3.5	1005	180.8	179.8	123.4	107.6	107.1

5.2.3. Effect of porous structure characteristics

The variation of the liquid fraction for different pore densities is displayed in Fig. 25 for the porosity of 95%. Similar to the melting process, the pore size has a negligible effect on the variation of liquid fraction. The results reveal that the porous medium with 50 PPI has the least liquid fraction at the same time.

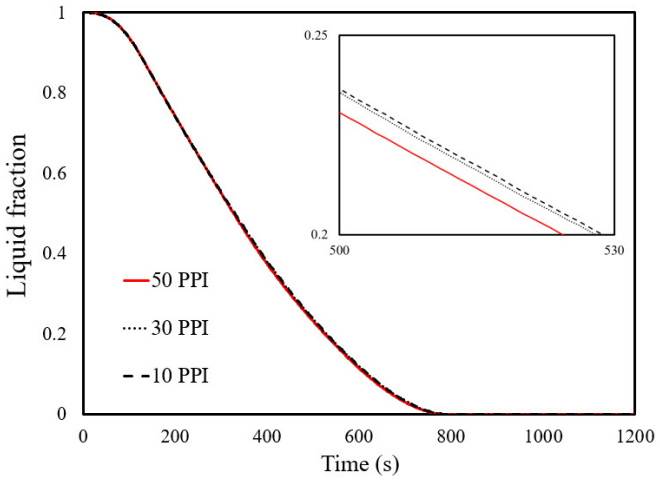

Fig. 25. The effect of pore size on the liquid fraction for the LHTES-W system with composite PCM in the solidification process.

The variation of the liquid fraction for the different porosity of copper foam is displayed in Fig. 26 for the pore size of 30 PPI in the solidification process. As expected, by increasing the porosity of the copper foam, the PCM solidifies in a longer time due to a lower rate of heat transfer. For the porosity of 98%, the solidification time in the LHTES-W system reduces by 91.3% compared with the pure PCM case.

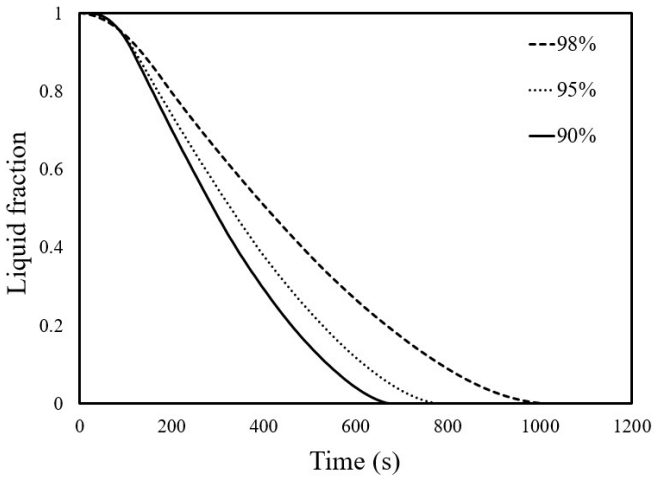

Fig. 26. The effect of foam porosity on the liquid fraction of the composite PCM inside the LHTES-W system in the solidification process.

5.2.4. Effect of HTF characteristics

Fig. 27 shows the effect of water inlet temperature in the solidification process on the liquid fraction of PCM inside the LHTES-W system with composite PCM at $A = 0.3$ and $L = 1.25$ with the porosity of 95% and pore size of 30 PPI. It is seen that the solidification time reduces by decreasing the water inlet temperature. By reducing the temperature from 290 K to 285 and 280 K, the solidification time decreases by 20.2% and 33.1% respectively.

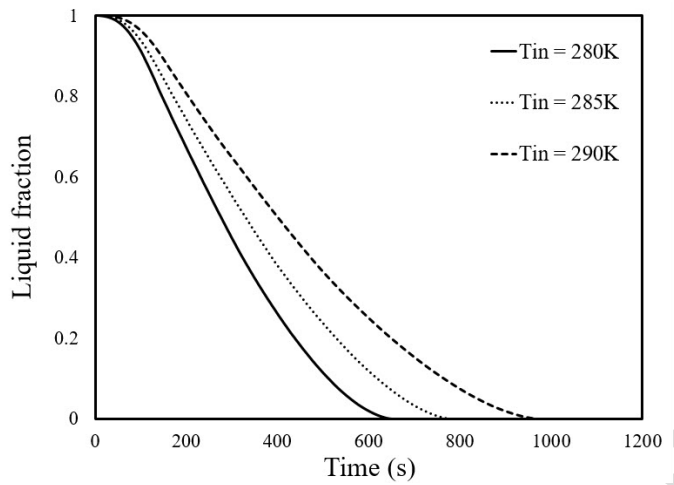

Fig. 27. The effect of inlet water temperature on the liquid fraction of the composite PCM inside the LHTES-W system in the solidification process.

Fig. 28 demonstrates the effect of Reynolds number in the solidification process on the liquid fraction of the composite PCM inside the LHTES-W system at $A = 0.3$ and $L = 1.25$. Similar to the melting process, higher Reynolds number results in a higher performance in the solidification process. It means that the solidification time decreases with increasing the Reynolds number due to the effects of the improved mixing of water and thereby, a higher heat transfer to the PCM container.

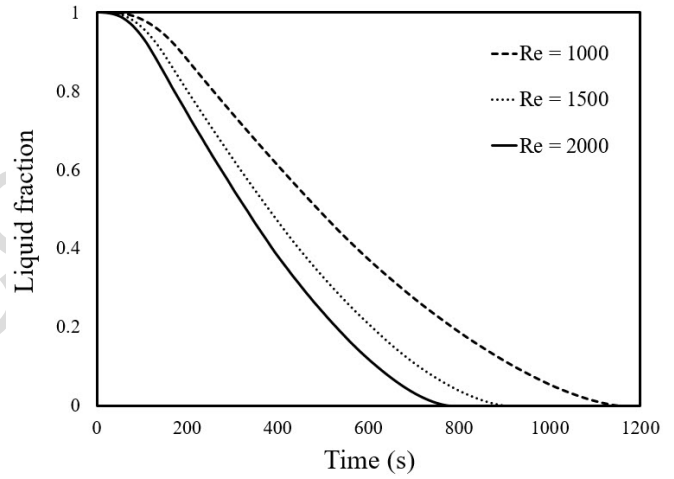

Fig. 28. The effect of water Reynolds number on the liquid fraction of the composite PCM inside the LHTES-W system in the solidification process.

6. Conclusion

In this study, the performance of a double-pipe latent heat storage unit with sinusoidal wavy channels using a composite copper foam-PCM is analysed in both melting and solidification processes. The results show the advantage of both channel waviness as well as adding porous structure inside PCM compared with the smooth channels system with pure PCM. The effects of wave amplitude, wavelength, porosity, pore size, inlet water temperature and water Reynolds number are studied comprehensively in melting and solidification process. The following outcomes are achieved through this numerical assessment:

- The solidification and melting times reduce by increasing the wave amplitude and Reynolds number and decreasing the wavelength.
- The higher rate of heat transfer to/from the PCM in the presence of the porous medium
- For the sinusoidal wavy channels LHTES unit with $L = 1.25$ and $A = 0.3$, the average rate of heat transfer is 192.8W and 236.2W for the melting and solidification processes, respectively, while it is 24.3W and 16.9W for the smooth channel case.
- For the LHTES-W system with $L = 1.25$ and $A = 0.3$, the melting and solidification times reduces by 88.7% and 93.3%, respectively compared with the wavy PCM alone system.
- The effect of channel waviness with $L = 1.25$ and $A = 0.3$ reduces the melting and solidification time by 24% and 25.5 compared with the smooth channel system for the composite system while it is 23.9% and 50% for the pure PCM system.

This paper provides guidelines for hybrid implementation of heat transfer enhancement methods including geometry modification as well as using a high conductive additive in Latent heat storage systems toward having a more beneficial storage unit.

References

[1] Khan Z, Khan Z, Ghafoor A. A review of performance enhancement of PCM based latent heat storage system within the context of materials, thermal stability and compatibility. Energy Conversion and Management. 2016;115:132-58.

[2] Zhou D, Zhao CY, Tian Y. Review on thermal energy storage with phase change materials (PCMs) in building applications. Applied Energy. 2012;92:593-605.

[3] Pereira da Cunha J, Eames P. Thermal energy storage for low and medium temperature applications using phase change materials – A review. Applied Energy. 2016;177:227-38.

[4] Merlin K, Delaunay D, Soto J, Traonvouez L. Heat transfer enhancement in latent heat thermal storage systems: Comparative study of different solutions and thermal contact investigation between the exchanger and the PCM. Applied Energy. 2016;166:107-16.

[5] Ge Z, Li Y, Li D, Sun Z, Jin Y, Liu C, et al. Thermal energy storage: Challenges and the role of particle technology. Particuology. 2014;15:2-8.

[6] Sushobhan BR, Kar SP. Thermal Modeling of Melting of Nano based Phase Change Material for Improvement of Thermal Energy Storage. Energy Procedia. 2017;109:385-92.

[7] Niu F, Ni L, Yao Y, Yu Y, Li H. Performance and thermal charging/discharging features of a phase change material assisted heat pump system in heating mode. Applied Thermal Engineering. 2013;58(1):536-41.

[8] Esapour M, Hosseini MJ, Ranjbar AA, Pahamli Y, Bahrampoury R. Phase change in multi-tube heat exchangers. Renewable Energy. 2016;85:1017-25.

[9] Al-Abidi AA, Mat S, Sopian K, Sulaiman MY, Mohammad AT. Internal and external fin heat transfer enhancement technique for latent heat thermal energy storage in triplex tube heat exchangers. Applied Thermal Engineering. 2013;53(1):147-56.

[10] Wang Y-H, Yang Y-T. Three-dimensional transient cooling simulations of a portable electronic device using PCM (phase change materials) in multi-fin heat sink. Energy. 2011;36(8):5214-24.

[11] Delgado M, Lázaro A, Mazo J, Zalba B. Review on phase change material emulsions and microencapsulated phase change material slurries: Materials, heat transfer studies and applications. Renewable and Sustainable Energy Reviews. 2012;16(1):253-73.

[12] Jamekhorshid A, Sadrameli SM, Farid M. A review of microencapsulation methods of phase change materials (PCMs) as a thermal energy storage (TES) medium. Renewable and Sustainable Energy Reviews. 2014;31:531-42.

[13] Sarı A, Karaipekli A. Thermal conductivity and latent heat thermal energy storage characteristics of paraffin/expanded graphite composite as phase change material. Applied Thermal Engineering. 2007;27(8):1271-7.

[14] Mills A, Farid M, Selman JR, Al-Hallaj S. Thermal conductivity enhancement of phase change materials using a graphite matrix. Applied Thermal Engineering. 2006;26(14):1652-61.

[15] Zhang P, Meng ZN, Zhu H, Wang YL, Peng SP. Melting heat transfer characteristics of a composite phase change material fabricated by paraffin and metal foam. Applied Energy. 2017;185:1971-83.

[16] Zhang H, Baeyens J, Cáceres G, Degrève J, Lv Y. Thermal energy storage: Recent developments and practical aspects. Progress in Energy and Combustion Science. 2016;53:1-40.

[17] Nomura T, Okinaka N, Akiyama T. Impregnation of porous material with phase change material for thermal energy storage. Materials Chemistry and Physics. 2009;115(2):846-50.

[18] Py X, Olives R, Mauran S. Paraffin/porous-graphite-matrix composite as a high and constant power thermal storage material. International Journal of Heat and Mass Transfer. 2001;44(14):2727-37.

[19] Mesalhy O, Lafdi K, Elgafy A, Bowman K. Numerical study for enhancing the thermal conductivity of phase change material (PCM) storage using high thermal conductivity porous matrix. Energy Conversion and Management. 2005;46(6):847-67.

[20] Mahdi JM, Nsofor EC. Melting enhancement in triplex-tube latent heat energy storage system using nanoparticles-metal foam combination. Applied Energy. 2017;191:22-34.

[21] Zhang P, Xiao X, Meng ZN, Li M. Heat transfer characteristics of a molten-salt thermal energy storage unit with and without heat transfer enhancement. Applied Energy. 2015;137:758-72.

[22] Esapour M, Hamzehnezhad A, Rabienataj Darzi AA, Jourabian M. Melting and solidification of PCM embedded in porous metal foam in horizontal multi-tube heat storage system. Energy Conversion and Management. 2018;171:398-410.

[23] Wang CC, Fu WL, Chang CT. Heat transfer and friction characteristics of typical wavy fin-and-tube heat exchangers. Experimental Thermal and Fluid Science. 1997;14(2):174-86.

[24] Jang J-Y, Chen L-K. Numerical analysis of heat transfer and fluid flow in a three-dimensional wavy-fin and tube heat exchanger. International Journal of Heat and Mass Transfer. 1997;40(16):3981-90.

[25] Shah RK, Sekulic DP. Fundamentals of Heat Exchanger Design: Wiley, 2003.

[26] Wang Q, Zeng M, Ma T, Du X, Yang J. Recent development and application of several high-efficiency surface heat exchangers for energy conversion and utilization. Applied Energy. 2014;135:748-77.

[27] Lotfi B, Sundén B, Wang Q. An investigation of the thermo-hydraulic performance of the smooth wavy fin-and-elliptical tube heat exchangers utilizing new type vortex generators. Applied Energy. 2016;162:1282-302.

[28] Kashani S, Ranjbar A, Abdollahzadeh M, Sebti S. Solidification of nano-enhanced phase change material (NEPCM) in a wavy cavity. Heat and Mass Transfer. 2012;48(7):1155-66.

[29] Abdollahzadeh M, Esmaeilpour M. Enhancement of phase change material (PCM) based latent heat storage system with nano fluid and wavy surface. International journal of heat and mass transfer. 2015;80:376-85.

[30] Agyenim F, Eames P, Smyth M. Heat transfer enhancement in medium temperature thermal energy storage system using a multitube heat transfer array. Renewable Energy. 2010;35(1):198-207.

[31] Wang P, Wang X, Huang Y, Li C, Peng Z, Ding Y. Thermal energy charging behaviour of a heat exchange device with a zigzag plate configuration containing multi-phase-change-materials (m-PCMs). Applied Energy. 2015;142:328-36.

[32] Nield DA, Bejan A. Convection in Porous Media: Springer International Publishing, 2017.

[33] Liu Z, Yao Y, Wu H. Numerical modeling for solid–liquid phase change phenomena in porous media: Shell-and-tube type latent heat thermal energy storage. Applied Energy. 2013;112:1222-32.

[34] Mat S, Al-Abidi AA, Sopian K, Sulaiman MY, Mohammad AT. Enhance heat transfer for PCM melting in triplex tube with internal–external fins. Energy Conversion and Management. 2013;74:223-36.

[35] Ye W-B, Zhu D-S, Wang N. Numerical simulation on phase-change thermal storage/release in a plate-fin unit. Applied Thermal Engineering. 2011;31(17):3871-84.

[36] Assis E, Katsman L, Ziskind G, Letan R. Numerical and experimental study of melting in a spherical shell. International Journal of Heat and Mass Transfer. 2007;50(9):1790-804.

[37] Xu Y, Ren Q, Zheng Z-J, He Y-L. Evaluation and optimization of melting performance for a latent heat thermal energy storage unit partially filled with porous media. Applied energy. 2017;193:84-95.

Highlights

- Study of a vertical double-pipe LHTES system with sinusoidal wavy channels
- Comparison of a composite metal foam-PCM LHS system with the pure PCM case
- Present the advantages of the porous medium on melting and solidification times
- Analysis of the distributions of liquid fraction and temperature and pressure drop
- Analysis of rate of transferred heat, TES rate, TES density and TES rate density